universität wien

MASTERARBEIT / MASTER'S THESIS

Titel der Masterarbeit / Title of the Master's Thesis

Effects of Climate Change on the Arctic Carbon Cycle

verfasst von / submitted by

Vinzent Klaus, B. Sc.

angestrebter akademischer Grad / in partial fulfilment of the requirements for the degree of

Master of Science (M. Sc.)

Wien, Juni 2017 / Vienna, June 2017

Studienkennzahl lt. Studienblatt / degree programme code as it appears on the student record sheet:	A 066 614
Studienrichtung lt. Studienblatt / degree programme as it appears on the student record sheet:	Metorologie
Betreut von / Supervisor:	ao. Univ.-Prof. Mag. Dr. Leopold Haimberger

Abstract

Due to multiple amplifying feedbacks, climate change is particularly pronounced in high northern latitudes. Therefore, the consequences of climate change on Arctic terrestrial ecosystems are particularly severe, raising the question, which role the Arctic will play in the future global carbon cycle. It is still unclear, if Arctic ecosystems will become a net carbon source under ongoing climate change, or if the stimulation of plant growth will offset carbon loss. After an introduction to the components of the carbon cycle and the control exerted by the climate, the features of Arctic tundra ecosystems are described. Moreover, the current state of research on high latitude climate change is summarised, and the most likely scenario of ecosystem consequences is presented. Furthermore, the results of a measurement campaign in Svalbard, which aimed to examine the effects of atmospheric warming on soil CO_2 efflux, will be described and discussed. Experimental long-term warming of the land surface resulted in an increase of soil CO_2 efflux, constituting a potential positive feedback to atmospheric warming. Measurements of primary production, which could have offset carbon release from the soil, were not conducted. Therefore, a point-level model simulation under different climate scenarios, using the Community Land Model (CLM) was run at the location of the study site. Adding a constant temperature factor to the atmospheric forcing resulted in a significant acceleration of biogeochemical reactions and amplification of carbon fluxes between ecosystem and atmosphere. A precipitation increase, which was simulated as well, tended to diminish both primary production and carbon release.

Zusammenfassung

Aufgrund einer Vielzahl an positiven Feedbackprozessen ist kaum eine Erdregion stärker vom derzeitigen Klimawandel betroffen als die hohen nördlichen Breiten. Die Auswirkungen des Klimawandels auf terrestrische Ökosysteme sind daher besonders drastisch, und werfen gleichzeitig die Frage auf, welche Rolle die Arktis im Kohlenstoffkreislauf zukünftig einnehmen wird; möglich ist sowohl, dass arktische Ökosysteme bei fortschreitendem Klimawandel eine Nettoquelle von Kohlenstoff werden, als auch, dass durch die Begünstigung des Pflanzenwachstums mehr Kohlenstoff gespeichert wird als verlorengeht. Im Zuge dieser Arbeit wird nach einer Vorstellung der Komponenten des Kohlenstoffkreislaufs und diesbezüglicher Besonderheiten der arktischen Tundra erläutert, warum der Klimawandel in hohen Breiten besonders ausgeprägt ist, und welche Folgen auf den arktischen Kohlenstoffkreislauf aus heutiger Perspektive wahrscheinlich sind. Zusätzlich werden die Ergebnisse einer Messkampagne in Spitzbergen, die die Untersuchung der Auswirkungen der atmosphärischen Erwärmung auf die Freisetzung von CO_2 aus dem Boden – die sogenannte Bodenatmung – zum Ziel hatte, im Detail vorgestellt und diskutiert. Eine experimentelle Langzeiterwärmung der Landoberfläche bewirkte einen Anstieg der Bodenatmung, was prinzipiell eine positive Rückkopplung zur Klimaerwärmung darstellt. Nicht beobachtet wurden jedoch die Auswirkungen auf die Kohlenstoffaufnahme, sodass eine Modellsimulation des Standorts in Spitzbergen unter verschiedenen Klimaszenarien mit dem Community Land Model (CLM) durchgeführt wurde. Eine künstliche Temperaturerhöhung führte zu einer signifikanten Beschleunigung der meisten Ökosystemprozesse und der Amplifikation sowohl der Kohlenstoffaufnahme von der Atmosphäre, als auch der -abgabe. Eine ebenfalls modellierte Zunahme des Niederschlags hatte hingegen dämpfenden Einfluss auf Primärproduktion und Kohlenstoffabgabe.

Contents

1 Introduction

Humans alter the physical and chemical properties of Earth's land surface, as well as its soils, atmosphere and biosphere since thousands of years through the change of surface cover, stock farming, agriculture and hunting, but only since the industrial revolution in the 18th century and the subsequent massive release of greenhouse gases in later centuries, these changes have been substantial enough to globally influence Earth's climate.

The current climate change poses one of the biggest environmental challenges and threats for humanity of our time. The average global temperature has already risen by approximately 0.9 °C since the late 19th century and is projected to continue increasing throughout the next decades (IPCC, 2013). An area particularly affected by climate change and its consequences are the high northern latitudes, where observations show a temperature increase far above average, and ecosystems are particularly sensitive to environmental changes. Therefore, scientists from many different fields have turned their focus on this part of the world in order to understand past changes in atmosphere, cryosphere, lithosphere, biosphere and hydrosphere that led to the pronounced climate change effects there. However, it is not only important to understand past changes, but to use this knowledge to predict future effects of a warming climate in high latitudes, because the consequences potentially affect the climate system on a global scale.

A particularly important process that could play a major role when assessing future Earth system changes is the flux of CO_2 from soils to the atmosphere, caused by autotrophic respiration by plant roots and heterotrophic respiration by microbial decomposition. Compared to the total amount of anthropogenic CO_2 emissions, soil respiration flux is about nine times higher on an annual basis and adds up to approximately 90 $PgC\,yr^{-1}$ (Hashimoto et al., 2015). As soil respiration rates typically increase with temperature, the additional CO_2 could further contribute to climate warming, especially in high latitudes, considering the pronounced temperature increase. Also, soils in high latitudes often contain vast amounts of organic carbon, most of it being stored in permafrost, not accessible for microbial decomposition. It is estimated that permafrost soils contain twice the amount of carbon currently present in the atmosphere as CO_2 (Schuur et al., 2008). With rising temperatures, this carbon reservoir

could become accessible to microbial decomposition and could ultimately be released to the atmosphere in the form of CO_2 and CH_4, representing another positive feedback for climate warming. Conversely, decomposition also releases nutrients, which are essential for plants in order to survive and grow. In combination with atmospheric warming, environmental conditions for plant growth could massively improve in the Arctic, favouring carbon sequestration in biomass, which would constitute a major negative feedback to climate change by fixing greenhouse gases from the atmosphere. Along with the greening of the Arctic, energy fluxes at the land surface would be altered, affecting meteorological processes and – as another feedback – climate.

While permafrost thawing and Arctic greening are likely the most prominent land feedbacks to climate change in high northern latitudes, many other interacting processes and feedbacks have been identified as well. Despite widespread scientific attention in recent years, projections of the future Arctic carbon balance are still relatively uncertain.

This thesis aims to provide an overview of the current state of research on the consequences of climate change for Arctic carbon cycling. Furthermore, results of a measurement campaign and point-level simulations in a polar semi-desert environment are used to illustrate climate change effects in a small valley in Svalbard.

2 Carbon cycle of the Arctic tundra

This chapter provides an overview of basic steps of terrestrial carbon cycling, illustrates special features of carbon fluxes and reservoirs in tundra ecosystems and summarises potential scenarios for the future of tundra carbon cycling under ongoing climate change.

2.1 General concepts of the terrestrial carbon cycle

2.1.1 Carbon uptake

Carbon and chemical energy enter ecosystems mostly by the process of photosynthesis, which is carried out by primary producers (autotrophs). Using light energy and water, inorganic, atmospheric CO_2 is reduced to organic compounds, releasing oxygen to the atmosphere as a waste product. The organic compounds obtained by photosynthesis are sugars, which can be stored, transported or metabolised in the plant (Chapin et al., 2011). Simultaneously to carbon fixation, the photorespiration reaction is catalysed, immediately releasing about 20 % to 40 % of the fixed carbon back to the atmosphere. This process is temperature-dependent; the proportion of respired carbon increases with temperature. Usually, when referring to photosynthetic carbon gain, the carbon loss by photorespiration is already subtracted.

Plants absorb CO_2 through little pores on the leaf surface, called stomata. There is an inevitable trade-off between CO_2 uptake and water loss, as larger stomata openings increase both the amount of CO_2 diffusing into the leaves and the amount of water lost by plant transpiration. Plants are able to actively influence this exchange of carbon dioxide and water by adjusting the size of their stomatal openings. Plants tend to regulate the openings in a way that carbon gain is maximised in high light, and water loss is minimised in low light. Nevertheless, other factors play a role as well, particularly the relative supplies of CO_2, water and nutrients. Water stress, for example, generally triggers a decrease in stomatal conductance.

On the ecosystem scale, the total amount of biomass gained by photosynthesis (excluding the carbon almost instantaneously lost by photorespiration) is referred to as gross primary production (GPP) – one of the most important measures of ecosystem productivity and land carbon uptake. There is considerable variation of GPP across ecosystems in different climate zones, and much of the variation can be attributed to photosynthetically active radiation (PAR), total leaf area and growing season length. The influence of the latter, as well as the controls that temperature, moisture and nutrient supply (primarily nitrogen and phosphorus) exert, are described below.

Temperature Low temperatures directly limit photosynthesis by reducing the rate of chemical reactions. With increasing temperature, photosynthetic activity – and GPP – increase as well, but only up to a certain point, because photorespiration rate rises faster than carbon uptake at high temperatures. In addition, warm conditions are often associated with high water losses by transpiration. However, direct temperature effects on photosynthesis are partly mitigated by evolutionary adaptations. In cold climates, plants produce leaves with high concentrations of nitrogen and photosynthetic enzymes, and raise the leaf temperature by morphological traits such as small hairs on the leaf surface.

Moisture As plants constantly lose water by transpiration, a relatively steady water supply is necessary to maintain photosynthesis. Abundant water resources are a key factor for the capability of plants to produce new leaves, and to support or increase leaf area in an ecosystem. As a result, GPP generally increases with precipitation.

Nutrient supply Photosynthesis requires large amounts of nitrogen for the production of photosynthetic enzymes. Therefore, leaf nitrogen concentrations correlate closely to photosynthetic capacity, which is defined as the photosynthesis rate per unit leaf mass (Wright et al., 2004). Excluding other parameters, GPP increases with rising nutrient concentrations in the soil.

Growing season length In many ecosystems, seasons that are too cold or dry to support significant photosynthesis occur. Plants respond to these periods in different ways: Annual plants die, others lose their leaves or become physiologically dormant. In any case, ecosystem carbon uptake is negligibly small outside of the growing season, and therefore, growing season length is an important determinant of GPP. Often, the photosynthetic season is defined by thresholds in temperature or moisture, above which photosynthesis is possible.

2.1.2 Carbon loss

There are many pathways of carbon loss from ecosystems, for example respiration of plants and animals, leaching of dissolved organic carbon or emission by wildfire. The largest carbon fluxes directed from terrestrial ecosystems to the atmosphere will be described in this chapter.

Autotrophic respiration

Even on plant level, carbon can be released in different ways, the by far most prominent being autotrophic (or plant) respiration, which serves to provide energy for growth, maintenance and ion absorption, and releases CO_2 to the atmosphere. Although autotrophic respiration of any plant increases with temperature, the effects of temperature are mitigated by acclimation and adaptation, so that plants in warmer environments have lower respiration rates at a given temperature than plants from colder climates, resulting in similar respiration rates for their average habitat temperature. For this reason, the fraction of GPP that is respired by plants is remarkably constant across ecosystems and climate zones, and is reported to range from 48 % to 60 % (Landsberg and Gower, 1997). Subtracting carbon loss by autotrophic respiration from carbon gained by photosynthesis gives the net primary production (NPP); the net carbon uptake by plants. Considering that the fraction of carbon lost by respiration is relatively constant, NPP is roughly half of GPP across biomes and climate zones.

$$NPP = GPP - R_{aut} \tag{2.1}$$

As gross primary production, NPP is measured at the ecosystem scale and averaged over an extended time period, most often a year. It is either specified as total biomass carbon gained (i.e., as gC) or mass of carbon taken up per unit area, and incorporates new biomass, as well as carbon transferred from the plant to the environment like soluble organic compounds secreted by roots, volatile organic compounds released by leaves and carbon transferred to microbes symbiotically associated with roots (Chapin et al., 2011).

The controls over NPP are almost identical to the factors controlling GPP (see section 2.1.1). The most dominant controls are growing season length and the availability of below-ground resources (moisture, nutrients). However, the latter are often regarded as indirect controls, as they are strongly influenced by the climatic parameters temperature and precipitation. NPP correlates strongly with precipitation, reaching highest values at 2000 mm to 3000 mm of

annual rainfall, before the effects of reduced oxygen availability in water-logged soils come into play. Given sufficient rainfall, NPP also correlates well with temperature.

Heterotrophic respiration

In contrast to autotrophic respiration, heterotrophic respiration is carried out by organisms that lack the ability to fix inorganic carbon and therefore rely on organic substrates as supply of chemical energy. Decomposition of dead organic material in the soil, mostly carried out by soil animals, is the major component of heterotrophic respiration in terrestrial ecosystems.

After dead organic matter – for example leaf and stem litter or animal residue – has reached the soil, the first step of decomposition is leaching of soluble materials into the environment, where they are either absorbed by microbes, react with soil minerals or are swept away and thereby lost from the system. Soil animals break up the remaining dead plant material and animal residue into smaller pieces, until it eventually becomes soil organic matter (SOM). With the aid of enzymes, soil microbes (fungi, bacteria and archaea) absorb and metabolise soil organic matter, releasing carbon dioxide (sometimes also other trace gases, depending on oxygen availability), inorganic nitrogen and recalcitrant compounds, which are resistant to further breakdown, as waste products (Klaus, 2016). Dead microbes eventually become part of soil organic matter themselves. The carbon stored in SOM is the largest carbon pool in terrestrial ecosystems (Post et al., 1982).

The main ecosystem consequence of decomposition is mineralization: The transformation of organic carbon and nutrients into inorganic matter such as carbon dioxide and ammonium. Worldwide, it accounts for approximately half of the CO_2 release from ecosystems. Furthermore, nitrogen mineralization by microbes is one of the most important steps in nutrient cycling (see section 2.1.4).

Due to the concentration of litter input near the soil surface, most decomposition and SOM formation occurs there. In most of Earth's ecosystems, decomposition and heterotrophic respiration above the soil surface are negligibly small. But which factors control decomposition rates? Allison (2006) distinguishes three main controls: Substrate quality, physical environment and the composition of the microbial community.

Substrate quality and quantity The susceptibility of litter to decomposition, termed substrate quality, varies widely between ecosystems and biomes. Generally, substrate quality in productive sites is higher, because plant-morphological traits that favour fast decomposition are supported by similar factors as NPP. Fast decomposition rates

are associated with large amounts of plant litter containing high concentrations of labile compounds and low concentrations of recalcitrant substances such as lignin. Decomposition is particularly enhanced near roots, since they excrete labile carbohydrates. The effects of nutrients on decomposition are often indirect, as they alter plant species composition and, in consequence, substrate quality. Nevertheless, the ratio of carbon to nitrogen (C:N ratio) in soils is a good predictor for decomposition rates, which are lowest in soils with high C:N ratio, i.e. high carbon and low nitrogen content.

Physical environment The most important physical controls of decomposition are moisture and temperature. Decomposition typically increases with soil water content because water films on soil surfaces support the diffusion of substrates to microbes (Stark and Firestone, 1995). Nonetheless, decomposition rates decline once soils become waterlogged due to the reduced availability of oxygen, which diffuses much slower through water than through air.

Temperature affects decomposition on several time scales. In the short term, heterotrophic respiration in the soil increases strongly with temperature due to enhanced enzyme activity. Microbial activity is also possible below 0 °C, because small quantities of water remain unfrozen, but it ceases below −12 °C (Mikan et al., 2002). Especially in the Arctic, microbial respiration in (mostly) frozen soils during the winter can be an important component of the year-round ecosystem carbon budget (Grogan, 2012).

On longer time scales, several other processes constrain temperature sensitivity. After a few weeks or months of elevated temperatures, microbes physiologically adjust to the warmed environment and down-regulate their activity (Bradford et al., 2008). On a similar time scale, the depletion of labile carbon pools in the soil may also play a role (Hartley et al., 2007). On even longer scales, increased temperatures may make carbon pools available for microbial decomposition that haven't been accessible before, as for example permafrost soils or wetlands (see section 2.3.1). In summary, the long-term effects of temperature on decomposition are far more complex than the exponential short-term response of microbial respiration would suggest.

Microbial community composition Differing from expectation, the total biomass of soil microbes has no significant impact on decomposition rates, it rather is a relatively constant fraction (about 2 %) of soil carbon mass (Chapin et al., 2011). However, a large fraction of microbes in the soil is inactive and therefore not directly involved in decomposition. What appears to be more relevant for decomposition rates is the

microbial community composition, as it affects the types and rates of enzyme production. While microbes that secrete enzymes breaking down regular compounds such as proteins are universally present in all soils, the microbial community composition can affect decomposition in ecosystems in which specific processes as methane production occur. As another example, only few microbes produce enzymes required for the breakdown of lignin, and do so only if nitrogen is unavailable. Additionally, oxygen is necessary during this process, therefore lignin is decomposed only in aerobic soils.

In wetlands, large amounts of organic material remain in a relatively undecomposed state due to lack of oxygen. Nevertheless, decomposition still occurs even in waterlogged soils, but at a significantly reduced rate. Microbes need electron acceptors to carry out redox reactions in order to satisfy their energy demands. Most microbes primarily use oxygen as acceptor, because energy gain is maximised that way, yet there are also other, energetically less favourable redox reactions with the following reactants, ordered by energy release to microbes:

$$O_2 > NO_3^- > Mn^{4+} > Fe^{3+} > SO_4^{2-} > CO_2 > H^+$$

Most microbes are specialised and perform only one or two redox reactions, facing a competitive advantage in environments where they are able to maximise their energy gain and where there is sufficient supply of their preferred electron acceptor. If oxygen is depleted, only those microbes that are able to transfer electrons from their food to other electron acceptors than oxygen can metabolise and grow (Chapin et al., 2011). In wetlands, oxygen concentrations that permit aerobic decomposition often occur solely close to the surface, while other reactions prevail in lower levels. Nitrate, another possible electron acceptor, is mostly unavailable in anaerobic soils, because the process providing nitrate, nitrification, requires oxygen itself. In freshwater wetlands, methanogens, which produce methane through a series of chemical reactions using inorganic carbon dioxide or bicarbonate as electron acceptors, predominate. Methane is highly reduced and therefore an excellent energy source for microbes in aerobic soil environments, as for example above the soil water table. A specific group of bacteria, methanotrophs, therefore consumes methane diffusing from deeper, anaerobic soil layers towards the atmosphere. This way, roughly two-thirds of total methane produced in anaerobic soils is oxidized before even reaching the atmosphere (Thauer, 1998). As a result, wetlands generally return more carbon dioxide than methane to the atmosphere. The proportion of methane emissions is greatest where methane can bubble to the surface, circumventing methanotrophs, for instance in ponds and lakes (Walter

et al., 2006). Roots and stems of some plants, for example sedges, provide another possible pathway to avoid oxidation (Verville et al., 1998).

Soil respiration

The release of CO_2 from soils to the atmosphere is commonly referred to as soil respiration, soil CO_2 efflux or soil CO_2 evolution. Technically speaking, soil respiration and the other terms should not be used interchangeably, as soil respiration refers to the production of CO_2 in the soil, while soil CO_2 efflux (or evolution) is the flux measured at the soil-atmosphere interface. On longer time scales as months or years, the difference is negligibly small though. Heterotrophic respiration by soil organisms and autotrophic respiration from roots account for most of the soil CO_2 production, and, to a lesser extent, chemical oxidation of carbon compounds and geological sources may contribute as well (Lloyd and Taylor, 1994). Observed soil CO_2 efflux rates are determined by soil CO_2 production, the CO_2 concentration gradient between soil and atmosphere, and other properties influencing the movement of CO_2 through and out of the soil such as soil pore size, temperature and wind speed (Raich and Schlesinger, 1992).

After gross photosynthesis, soil respiration is the second-largest terrestrial carbon flux, and the largest flux directed from land to the atmosphere. Estimates of global R_s, as soil respiration rate is abbreviated most often, range from 68 $PgC\,yr^{-1}$ (Raich and Schlesinger, 1992) to 98 $PgC\,yr^{-1}$ (Bond-Lamberty and Thomson, 2010), implying relatively high uncertainty. The uncertainty is also highlighted by large variations in Earth system model outputs of soil carbon stocks and heterotrophic respiration (Hashimoto et al., 2015). Compared to anthropogenic carbon emissions from burning fossil fuels and cement production, which add up to approximately 8 $PgC\,yr^{-1}$, R_s is ten times larger, and due to its temperature and moisture sensitivity also considered to be an important feedback for climate change. Furthermore, knowledge of soil respiration rates is critical for estimating soil carbon turnover, and allows examination of microbial activity, nutrient cycling and other soil processes.

Since soil respiration is the combined effect of autotrophic root respiration and heterotrophic microbial respiration, spatio-temporal variations can be attributed to the same factors that influence these two types of respiration. Hence, the major controls are soil temperature, moisture and substrate quality and quantity. In absence of soil moisture limitations, soil respiration rates increase with warming over the range of temperatures typically encountered in a particular ecosystem, but soil respiration at a given temperature varies widely between ecosystems, in most cases due to differences in substrate quality and quantity. Highest soil

respiration rates are observed in warm and moist environments, where both the physical environment and the litter input are favourable, and approach zero below −12 °C (Raich and Tufekciogul, 2000). Additionally, soil factors like soil drainage and plant root density, and plant parameters as root nitrogen concentration are influential (Grant and Rochette, 1994).

Across biomes, there is a strong positive correlation between annual NPP and soil respiration due to the tight linkage between the two processes (Raich and Tufekciogul, 2000). Plant litter and root exudations provide carbon input for microbial decomposition and roots directly respire in the soil, both processes producing soil CO_2. Vice versa, decomposition controls nitrogen mineralization and, consequently, nutrient availability, which affects plant production (Reich et al., 1997). The magnitude of both effects is influenced by temperature and moisture. In seasonal environments, often two annual peaks of soil respiration rates can be observed: The first one during summer, when temperatures, decomposition rates and root exudations are highest. In autumn, litter input from senescence often causes a second peak of decomposition and, subsequently, soil respiration.

For evaluating the temperature dependency of soil respiration, observation-based first-order exponential relationships without theoretical background are widely used:

$$R_s = Ae^{BT} \tag{2.2}$$

Here, A and B are constants obtained by regression analysis of observational data, and T usually is soil temperature, although air temperature is sometimes used instead, depending on data availability. It is known that this formulation slightly underestimates respiration at low temperatures and overestimates it at high temperatures (Lloyd and Taylor, 1994). Another Arrhenius type fit suggested by Lloyd and Taylor accounts for this effect:

$$R_s = A' e^{\frac{-B'}{T-T_0}} \tag{2.3}$$

This fit requires one additional model parameter, T_0. However, other studies could not confirm significantly better fits by using equation 2.3 (Leirós et al., 1999; Fang and Moncrieff, 2001). The reason may lie in the range of temperatures available from observations. If the range between lowest and highest temperature in the dataset only spans up to 20 K, first-order exponential fits seem to be sufficient (Mikan et al., 2002).

In the context of temperature dependencies, the Q_{10} value is an important index. It is used to express the temperature response of various biological and chemical systems, and quantifies the proportional change of a process rate caused by a temperature increase of 10 °C. Applying it to soil respiration rates yields:

$$Q_{10} = \left(\frac{R_2}{R_1}\right)^{\frac{10}{T_2 - T_1}} \tag{2.4}$$

If a regular first-order exponential fit (eq. 2.2) for observational data is applied, Q_{10} can be rewritten as:

$$Q_{10} = e^{10B} \tag{2.5}$$

Unsurprisingly, this type of fit corresponds to constant Q_{10}, in contrast to Lloyd and Taylor's equation that allows variation of temperature dependency. Normally, Q_{10} is somewhat higher for low temperatures and decreases with increasing temperature, conforming with the finding that eq. 2.2 minimally under- or overestimates measured soil respiration rates, depending on temperature. Q_{10} typically varies between 1.5 and 7 across ecosystems for soil temperatures above freezing point, while particularly high values around 100 are observed at temperatures below 0 °C (Mikan et al., 2002).

Other forms of carbon loss

While autotrophic and heterotrophic respiration are typically the dominant pathways of carbon loss from ecosystems, there are also other carbon fluxes that can be notable under certain conditions.

Gaseous carbon fluxes Since the industrial revolution, anthropogenic emissions of gaseous carbon forms have drastically increased and constitute a considerable carbon flux nowadays: Carbon release from fossil fuel combustion and cement production added up to roughly 9.5 $\mathrm{PgC\,yr^{-1}}$ in 2011, equivalent to 7 % to 8 % of total ecosystem respiration and wildfire emissions (IPCC, 2013). Aside from that, there are also large natural fluxes not associated with autotrophic and heterotrophic respiration: Plants sometimes emit carbon in other forms than CO_2, most notably volatile organic compounds like the major class of terpenes. Moreover, significant amounts of carbon dioxide are infrequently emitted by wildfires. Carbon loss may be equivalent to up to 30 % of

NPP in fire-sensitive ecosystems such as the Canadian boreal forest (McGuire et al., 2010). Besides CO_2, wildfires also release larger amounts of carbon in form of carbon monoxide.

Dissolved carbon fluxes Leaching of dissolved organic carbon (DOC) and dissolved inorganic carbon (DIC) to groundwater and rivers can be substantial in some ecosystems, especially in those with high annual precipitation sums.

Particulate carbon fluxes Transfers of particulate carbon largely result from lateral movements of carbon by erosion and wind deposition, which can be quantitatively important in case of extreme events such as floods. The anthropogenic influence is significant in heavily populated areas, and in lands used for agriculture and forestry, as human harvests are often shipped over long distances and large numbers of trees are removed from forests. In general, however, particulate carbon fluxes are relatively small and are therefore often neglected.

2.1.3 Carbon balance

The carbon balance of an ecosystem is largely determined by photosynthesis on the one hand, and carbon release to the atmosphere by autotrophic and heterotrophic respiration on the other hand. Subtracting autotrophic and heterotrophic respiration from gross primary production gives the net ecosystem production (NEP).

$$NEP = GPP - R_{aut} - R_{het} = NPP - R_{het} \tag{2.6}$$

The sum of R_{aut} and R_{het} is often termed ecosystem respiration, R_{eco}. Both gross primary production and ecosystem respiration are very large fluxes whose difference is relatively small. Therefore it is difficult to assess NEP, but there is a similar quantity that is often used as an approximation and can be measured more easily: Net ecosystem exchange (NEE), which is defined as net exchange of CO_2 between ecosystem and atmosphere, and is, contrary to NEP, by convention positive if CO_2 is released from the ecosystem to the atmosphere.

Plant production and ecosystem respiration are closely linked, because both plant and microbial respiration depend on carbon input from primary production, and primary production depends on microbial nutrient processing. Still, plant production and ecosystem respiration are rarely balanced, and NEP is the result of factors that contribute to this imbalance (Chapin et al., 2011). Imbalances occur on various time scales; for example, photosynthetic carbon

gain tends to exceed carbon loss by respiration during daytime and vice versa during the night; a similar pattern is observed in the majority of seasonal environments between summer (NEP > 0) and winter (NEP < 0), because microbial activity is supported over a broader temperature range than plant growth. On longer time scales, time since disturbance influences NEP. Immediately after ecological disturbances such as wildfires, weather extremes or human harvests, biomass and GPP are significantly reduced, while respiration may be diminished, but ongoing, causing NEP to be negative. However, GPP recovers relatively fast, as conditions early after disturbances normally favour plant growth, and eventually GPP exceeds ecosystem respiration. After several years, heterotrophic respiration catches up with GPP due to the slowdown of plant growth. In general, the more time has passed since the disturbance, the less pronounced the imbalance will be.

Imbalances are also prevalent in wetlands: Plant growth and, eventually, NPP are less affected by waterlogged soils and oxygen depletion than microbial activity is, because many plants adapted to these environments are able to transport oxygen acquired by leaves to their roots (Chapin et al., 2011). Accordingly, wetlands in all latitudes generally accumulate soil organic matter; approximately one-third of Earth's SOM is stored in wet soils (Schlesinger, 1997).

Still, there is no clear relationship between NEP and climate as both plant production and respiration are generally favoured by the same climatic conditions. It is possible that NEP is largely insensitive to climate, and the main determinant is successional stage after disturbance (Luyssaert et al., 2007). However, it is likely that climate change alters the balance between the components of NEP both directly and through a series of side effects, and there is indication that global NEP is already being stimulated by warming, higher atmospheric CO_2 concentrations – and massive anthropogenic nitrogen input (Heimann and Reichstein, 2008). This might be the explanation for positive NEP measurements across a wide range of ecosystems, although another plausible reason could be that most ecosystems are still in succession after a disturbance, and steady state is seldom reached, even decades or centuries after disturbances (Luyssaert et al., 2007; Xiao et al., 2008).

NEP and NEE don't incorporate all types of carbon fluxes to and from ecosystems and are therefore insufficient to quantify the full carbon balance. The change of carbon mass in an ecosystem is termed net ecosystem carbon balance, and includes all possible carbon fluxes in gaseous, particulate or dissolved form:

$$NECB = \frac{dM_C}{dt} \tag{2.7}$$

Rewriting this equation by specifying the carbon fluxes yields:

$$NECB = \underbrace{(-NEE + F_{CO} + F_{CH4} + F_{VOC})}_{\text{gaseous inputs/losses}} + \underbrace{(F_{DIC} + F_{DOC})}_{\text{dissolved inputs/losses}} + \underbrace{F_{POC}}_{\text{particulate inputs/losses}} \quad (2.8)$$

Here, F_{CO} denotes the carbon monoxide flux, F_{CH4} the methane flux, F_{VOC} is the flux of volatile organic compounds, F_{DIC} is the transfer of dissolved inorganic carbon, F_{DOC} is the transfer of dissolved organic carbon, and F_{POC} is the transfer of particulate organic carbon. Similar to NEP, NECB depends largely on the successional stage after disturbances (apart from wetlands), with significant carbon accumulation occurring during the first years after a disturbance.

2.1.4 Nutrient availability

Plants require nutrients for survival and growth. Terrestrial nutrient and carbon cycles are coupled tightly through the fundamental role that nutrients play for plant productivity. Changes in nutrient cycles affect the carbon cycle and vice versa. Out of all nutrients, nitrogen generally plays the most important role, as it is needed in largest amounts and limits plant growth in many ecosystems around the world. It is generally cycled tightly within ecosystems, particularly if they are nutrient-poor (Chapin et al., 2011). Plants cannot access the vast atmospheric nitrogen pool directly and depend mostly on acquisition from the soil, where nitrogen is enriched by microbial recycling from nitrogen-containing litter and atmospheric deposition. Additionally, significant amounts of nitrogen enter ecosystems by nitrogen-fixing bacteria, which convert atmospheric di-nitrogen to ammonium; an energetically expensive process sometimes carried out in symbiotic relationship with plants, because they can provide the carbohydrates needed to meet the energy demand. Nitrogen fixation is favoured by warm, tropical environments, and relatively small in high latitude ecosystems (Houlton et al., 2008).

Analogous to the distribution of carbon in ecosystems, nutrient pools are separated into aboveground biota, below-ground plant parts, dead organic matter and inorganic reservoirs. In the soil, the vast majority of nitrogen is contained in dead organic matter and is therefore inaccessible to plants. In the course of decomposition, microbes release different forms of nitrogen – dissolved organic nitrogen and inorganic ammonium, the latter by the process of mineralization – that can be absorbed by plant roots.

2.2 Characteristics of Arctic tundra

Tundra is a type of biome characterized by harsh climatic conditions that inhibit tree growth. Leaving aside Antarctic and alpine tundra, this thesis will focus entirely on Arctic tundra. This tundra type covers approximately 8 % of Earth's land surface. To the south, it is bordered by boreal forest (taiga), to which a transitional zone up to several hundred kilometres wide exists, and to the north, it is limited solely by the Arctic Ocean. From south to north, several types of tundra are distinguished: Forest tundra – a somewhat paradoxical term – directly north of the transition zone to taiga is followed by the low Arctic, the southernmost zone with tundra vegetation in a strict sense, in this case dominated by shrubs and sedges. Further northwards (>70°N) is the high Arctic, where polar semi-desert communities with cryptogams and herbs occur in the south, and less than 5 % of the ground surface are covered by vegetation in the polar desert of the far north (Callaghan et al., 2005).

2.2.1 Climate

The description of tundra climate is often based on the classification by Köppen (1931): The average temperature of the warmest month is lower than 10 °C, but higher than 0 °C. Anyway, there is considerable variation of temperatures within the tundra biome, and average July temperatures range from 10 °C to 12 °C at the southern boundary to 1.5 °C in polar deserts. Accordingly, the length of the growing season declines from 3.5 months at southern sites to 1.5 months in the far north (Callaghan et al., 2005). Solar input varies considerably between summer and winter, as a large part of the tundra biome is located north of the Arctic Circle at 66.5°N, where midnight sun and polar night occur. Therefore, solar radiation input in winter is practically zero, while it is relatively high in summer. However, due to the high albedo of snow and ice, large parts of the summer radiation are reflected at the surface in polar areas. Pronounced temperature inversions are a common feature of the lower troposphere in the Arctic winter, particularly in continental regions, due to the vast loss of heat by longwave radiation at the surface.

Differences between regional climates in the Arctic are pronounced and largely controlled by ocean currents and atmospheric pressure patterns – both of which cause massive fluxes of energy, moisture and momentum – in combination with the continentality of a specific site. Cold ocean currents originate from Arctic waters, where the energy deficit is largest. They are for instance found along Canada's east coast, while warm currents flow northwards in the eastern parts of the Pacific and Atlantic ocean. Characteristic surface air pressure

patterns of the northern hemisphere in winter are the Aleutian and the Icelandic low and the continental Siberian high, while the pressure distribution in summer is dominated by the subtropic highs in the northern Atlantic and Pacific and low gradients across Arctic and subarctic areas. Regarding seasonal cycles in the Arctic, average sea-level pressure is highest in late spring with a secondary maximum in autumn, and lowest in winter (McBean et al., 2005). As these climatological pressure patterns reflect the tracks of moving cyclones, which carry heat, moisture and momentum, low average pressure is generally associated with enhanced precipitation.

The dominating mode describing interannual climate variability is the Arctic Oscillation (AO), a pattern derived by empirical orthogonal function (EOF) analysis of sea-level pressure anomalies in the northern hemisphere that is related to the North Atlantic Oscillation (NAO). The time series of principle components of this mode (see Fig. 2.1) is referred to as Arctic Oscillation Index (AOI) and explains approximately 20 % to 30 % of the variance of sea-level pressure in the northern hemisphere (McBean et al., 2005). Positive AO indices correspond to strong westerly flows in mid-latitudes and negative pressure anomalies in high latitudes (particularly in the area of Iceland), while the polar vortex is weaker and more distorted during phases of negative AOI. Moreover, cyclone activity tends to be shifted polewards during high AOI, favouring warm air advection in many polar regions, especially in the eastern Arctic Ocean and over northern Eurasia (Rigor et al., 2000).

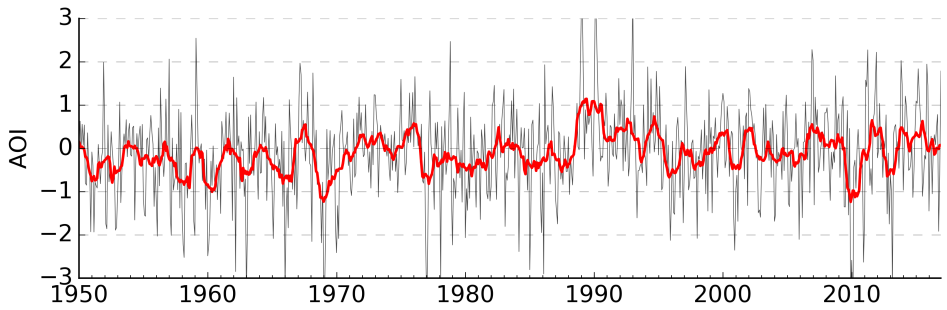

Figure 2.1: Monthly mean (thin black line) and 12-month running mean (red line) of the Arctic Oscillation Index between 1950 and 2016. The data is based on NCEP/NCAR reanalysis and was downloaded from the NOAA website.

The physical causes of AOI long-term trends are disputed, but seem to be related to sea surface temperature changes in the North Atlantic (Rodwell et al., 1999) and in the tropics (Hoerling et al., 2001).

As a result of regional climate patterns, the southern boundary of Arctic tundra varies considerably around the globe; while tundra vegetation at low altitudes can be found in eastern

Canada already at 51°N, boreal forest extends up to 69°N in Norway. To the north, tundra extends up to 84°N, as there is no landmass beyond that latitude. Annual precipitation is subject to considerable variation within high latitudes, ranging from 45 mm in northern polar desert to 1100 mm in northern Norway.

2.2.2 Vegetation

Plant biomass and species diversity are low, and progressively decline towards the north. In total, Arctic tundra is home to approximately 1800 vascular plants and 4000 cryptogams such as mosses (Callaghan et al., 2005). While shrubs and robust trees like spruce and birch dominate at the southern boundary, mostly herbs, lichens and mosses are found in the high Arctic. Plant species growing in Arctic tundra have to cope with extreme environmental conditions: Very low temperatures, a short growing season, poor nutrient availability and frequent mechanical disturbances such as freeze-thaw cycles or heavy snow loads. Plants are adapted to the harsh environment by slow growth, long life cycles and a low stature.

2.2.3 Soil respiration

Typical soil CO_2 efflux rates in tundra ecosystems obtained in various field measurements are in the magnitude of 60 $gC\,m^{-2}\,yr^{-1}$; however, there is considerable spatio-temporal variation (Raich and Schlesinger, 1992). Small-scale and regional differences can be attributed to variations of temperature – Q_{10} values in Arctic soils are relatively high -, soil moisture, and furthermore to vegetation types due to differences in litter quality, root production and root respiration. The proportion of soil CO_2 efflux attributable to root respiration is particularly high in Arctic tundra, ranging from 50 % to 93 % (Billings et al., 1977). Plants exert influence both during summer and winter (Grogan and Chapin, 1999; Grogan, 2012).

Growing season respiration rates are well-documented since decades, but in recent years it became evident that substantial biological activity and consequently respiration in the soil are sustained during the Arctic winter as well, accounting for 15 % to 50 % of annual respiration (Grogan and Jonasson, 2006). Snow cover affects wintertime respiration by thermal insulation of the soil against low air temperatures, thus increasing soil temperature and respiration during most of the cold season. Grogan (2012) points out that peak snow depth correlated well with total winter soil respiration in his experiment. Thereby, shrub cover can indirectly affect wintertime soil respiration: Interactions between drifting snow and shrubs typically increase snow depth within and downwind of shrubs, in consequence

elevating soil temperatures and respiration rates (Sturm et al., 2001). Snow is trapped by the reduction of wind speeds, and sublimation of fallen snow is reduced as well. But which effects are caused by the snow cover in spring, when air temperatures rise and insulation effectively reduces soil temperature, at least during the daytime? Snow melt in high latitudes occurs late during the season, and by the time the last centimetres of snow are melted away, it is a rather fast process as solar input is already close to its maximum. As a result, the period of snow cover is extended only for a few days in shrub areas despite their increased accumulation of snow, and the potential reduction of soil temperature during that time span cannot offset the effects of increased soil temperature during large parts of the winter (Nobrega and Grogan, 2007).

In the course of the spring snow melt, often short, large bursts of soil CO_2 that has accumulated below the snow cover are released (Elberling and Brandt, 2003). Especially in moist, poorly drained soils, CO_2 can be trapped effectively while the soil is frozen and covered with snow, causing a decoupling of CO_2 production in the soil and its release to the atmosphere. Additionally, freeze-thaw cycles in spring are accompanied by pulses of increased soil respiration. They are produced by the metabolism of organic substrates released by the death of microbes (Schimel and Clein, 1996).

2.2.4 Carbon Balance

Carbon fluxes in the Arctic tundra are smaller than in most other ecosystems, because rates of biogeochemical processes are restricted by the extreme environmental conditions: Carbon uptake by plants is limited by the cold climate, the short growing season and little amounts of plant-accessible nutrients; carbon loss by respiration, in turn, is strongly constrained by the small plant biomass as well as by low temperatures, which slow down decomposition. On account of this, the carbon cycle as a whole is relatively slow. Nevertheless, tundra ecosystems have, on average, acted as a carbon sink for the past 10000 years (Pries et al., 2012). Observations and process-based models indicate that Arctic tundra is still a carbon sink on multi-year time scales, however, large uncertainties remain to which extent. Synthesizing data from various sources, McGuire et al. (2012) estimated a tundra NEP of 110 $\mathrm{TgC\,yr^{-1}}$ between 1990 and 2006, with a confidence interval ranging from a weak carbon source of $-80\ \mathrm{TgC\,yr^{-1}}$ to a relatively strong carbon sink of 291 $\mathrm{TgC\,yr^{-1}}$. Based on an analysis of observations in 32 sites between 1990 and 2006, Belshe et al. (2013) found tundra to be a weak source of CO_2, but they explicitly excluded data from fens, bogs and mires in their study, which most likely caused the discrepancy to McGuire's estimate. Uncertainties regarding the

carbon balance are generally high for far northern latitudes, because larger, ground-bases observation networks measuring CO_2 fluxes have been established only in recent years. Sink activity could have increased since the 1990s, but it is possible that this apparent trend is an artefact resulting from biased observations in the 90s (McGuire et al., 2012). However, Oechel et al. (2000) reported that tundra might have been a carbon source in the 1970s and 80s, corresponding well with McGuire's result.

In poorly drained, anaerobic soils of tundra wetlands, microbial decomposition is more strongly inhibited than plant growth (Oechel et al., 2000; Post et al., 1982). As a consequence, wet tundra ecosystems are long-term carbon sinks and slowly accumulate carbon in their soils, while drier tundra sites have more balanced carbon budgets. Differences in net carbon uptake between wet and dry tundra ecosystems occur mainly during the growing season, while there are no significant differences during winter, when all tundra soils are sources of CO_2 due to lack of photosynthesis. As a result of the sink activity in summer, highest soil carbon stocks have accumulated in wet tundra ecosystems, particularly in peatlands. In contrast, significantly less carbon is sequestered in dry tundra ecosystems, for example in polar deserts and semi-deserts (Horwath and Sletten, 2010).

Compared to temperate and tropical ecosystems, little carbon is stored in plant biomass, mainly because of low productivity and lack of tree growth. Moreover, most of the plant biomass is allocated belowground to roots. Plant biomass and primary production progressively decrease from south to north due to the decline in growing season length and temperatures. In contrast to the vegetation pool, the total soil carbon stock is vast, because of the large extent of carbon-accumulating wetlands in Arctic tundra. The amount of soil organic matter is lower at far northern latitudes, in polar deserts and semi-deserts, as well as in drier ecosystems near the southern boundary. However, latitudinal variation of carbon stocks of the same ecosystem type is often less pronounced than variation among ecosystem types within one region, where soil organic matter content and primary production can vary by more than three orders of magnitude (Jonasson et al., 2001). This pattern suggests that landscape-scale variations in environment – particularly microtopography and hydrology – and disturbance regime are more influential controls on the spatial distribution of carbon sequestration than large-scale climate.

Unsurprisingly, annual methane emissions are greatest in wet tundra sites, with highest fluxes observed during the growing season. Between 1990 and 2006, there was an estimated net CH_4 release to the atmosphere of 19 $\mathrm{TgC\,yr^{-1}}$, with an uncertainty range between 8 $\mathrm{TgC\,yr^{-1}}$ and 29 $\mathrm{TgC\,yr^{-1}}$ (McGuire et al., 2012).

As in most ecosystems, autotrophic and heterotrophic respiration are the dominant pathways of carbon loss. Considering that NEP is close to neutral, however, other pathways become significant for the total carbon budget. Aquatic losses of dissolved organic and inorganic carbon to the ocean are notable, because they may add up to 80 $TgC\,yr^{-1}$ (McGuire et al., 2009). Dissolved organic carbon reaching lakes is eventually consumed by aquatic microbes and also released to the atmosphere, mostly in the form of CO_2 (Callaghan et al., 2005). Furthermore, large wildfires sometimes release carbon in the magnitude of a few teragram per event (Mack et al., 2011).

2.2.5 Nutrient availability

In Arctic tundra, the soil nitrogen pool is significantly larger than the reservoir of nitrogen stored in plants, resembling the distribution of carbon (Jonasson and Michelsen, 1996). Rates of nitrogen input and output are generally low, resulting in a relatively closed cycling of nutrients (Callaghan et al., 2005). Furthermore, nitrogen cycling is very slow compared to other ecosystems, because of low decomposition rates and little plant production. Despite the relatively large soil nitrogen pool and little demand because of low GPP, tundra ecosystems are sensitive to fertilization, indicating nitrogen limitation. This is because most nitrogen in the soil is unavailable to plants; also a consequence of slow microbial decomposition, which could make it accessible. Besides nitrogen, phosphorus is another major nutrient, which tends to be the limiting nutrient in wet ecosystems, while dry and mesic sites are primarily limited by nitrogen (Jonasson et al., 2001). Compared to other ecosystems, plants in the tundra acquire nitrogen to a remarkable extent in its dissolved organic form, a result of the pronounced limitation (Chapin et al., 2011).

2.2.6 Permafrost

Most parts of Arctic tundra are underlain by permafrost, which is defined as "soil, rock, sediment or other Earth material with a temperature that has remained below 0 °C for two or more consecutive years" (Walsh et al., 2005). Permafrost areas are categorised into continuous, discontinuous and sporadic, depending on the proportion of soil occupied by permafrost in a specific area. In continuous permafrost zones, all of the soil is underlain by permafrost, whereas permafrost underlies 10 % to 90 % of the soil in discontinuous and sporadic permafrost. The boundary between discontinuous and sporadic is not rigorously defined, but commonly regions in which permafrost underlies less than 30 % to 50 % of

the land area are considered to belong to the sporadic permafrost zone. Permafrost is not restricted to tundra, as it reaches far south of the treeline. It is documented below 50°N in Mongolia (Sharkhuu, 2003), and even further south in alpine sites. In total, 12.8 % to 17.8 % of the exposed land area in the northern hemisphere is underlain by permafrost (Zhang et al., 2000).

The surface layer of the soil that is seasonally unfrozen is called active layer, which is where most biogeochemical processes occur. Maximum active layer depth varies between several tens of centimetres and one to two metres, depending on ground heat flux. A vegetation cover and belowground organic layers reduce the thermal diffusivity of the soil, attenuating the influence of atmospheric temperatures on the soil and keeping permafrost cooler during summer than without vegetation. Additionally, evapotranspiration and melting remove latent heat.

While permafrost can reach depths of several hundred metres, organic carbon is generally confined to the upper 25 m of soil, normally with highest concentrations near the surface. The carbon reservoir in permafrost is tremendous, as organic material accumulated over thousands of years without being depleted by microbial decomposition. Recent estimates quantify carbon storage in circumpolar permafrost regions of the northern hemisphere with (1035 ± 150) PgC in the surface 3 m of soil, about 50 % of the global soil carbon pool in this layer (Schuur et al., 2015). Deeper soil layers contain considerable amounts of frozen organic matter as well: For yedoma soils, which are ice-rich, perennially frozen soils in Alaska and Russia present since the last Ice Age, two notable, but differing estimates of carbon pool size were published in the past few years, ranging from (210 ± 70) PgC (Strauss et al., 2013) to (456 ± 45) PgC (Anthony et al., 2014). The difference may stem from diverging assumptions regarding ice content and sediment depth. Permafrost soils in the major Arctic river deltas contain additional (91 ± 39) PgC (Hugelius et al., 2014). Besides yedoma soils and river deltas, other permafrost regions contain deep carbon too, but due to sparse data availability, only a rough estimate of 350 PgC to 465 PgC of additional carbon can be made (Schuur et al., 2015). In total, the known pool of carbon in northern permafrost regions adds up to 1330 PgC to 1580 PgC, with a potential additional pool of roughly 400 PgC.

2.3 Climate change in Arctic tundra

Climate change due to anthropogenic greenhouse gas emissions and land-use changes is augmented in Arctic regions by several positive feedback effects, leading to a temperature

increase in recent decades that is at least twice as large as on global average (see Fig. 2.2); a phenomenon known as Arctic amplification (IPCC, 2013).

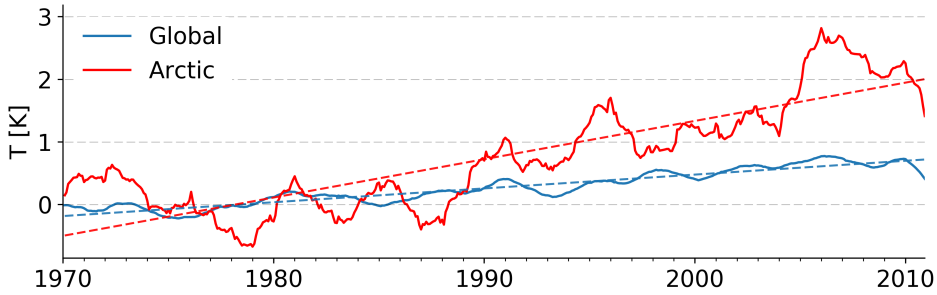

Figure 2.2: Time series of global and Arctic (>66.5°N) surface temperature anomalies relative to the reference period 1961-1990, smoothed by a 24-month running mean (solid lines). Dashed lines indicate the linear trend between 1970 and 2010. The data is based on the ERA-20C reanalysis and was downloaded from the ECMWF homepage.

The dramatic sea ice loss – the areal extent of summer sea ice decreased by 50 % since 1979 (Vihma, 2014) – and, to a lesser extent, the reduction of snow cover over land in spring, triggered the surface albedo feedback, one of the main drivers of Arctic amplification, as absorption of solar radiation at the surface is increased; thereby reinforcing warming, sea ice retreat and snow cover decrease (Screen and Simmonds, 2010; Taylor et al., 2013). In summer, most of the additional energy is used to warm the upper ocean, until a part of the heat is subsequently released to the atmosphere in autumn and winter, when air temperatures drop below sea surface temperatures, reversing the heat flux between ocean and atmosphere (Mayer et al., 2016). Since isolating sea ice is missing, the flux can be particularly large. As a result, Arctic warming is most pronounced in autumn and winter, and in areas affected by sea ice loss (see Fig. 2.3). Due to the typically very stable surface inversion during the Arctic winter, vertical mixing in the boundary layer is restricted and the warming cannot be mixed to upper levels, causing particularly strong near-surface warming (Bintanja et al., 2012).

Increasing evaporation and specific humidity due to sea ice retreat and rising temperatures pose another potential feedback, as water vapour is a powerful greenhouse gas. Observational studies have also indicated larger poleward moisture transport by changes in the atmospheric circulation due to more frequent meridional wind patterns (Overland and Wang, 2010; Zhang et al., 2013). Moreover, additional moisture potentially increases cloud cover, which may also contribute to warming, depending on cloud height and season.

The radiation emitted from a black body is highly nonlinear with respect to temperature, as described by the Stefan-Boltzmann law. Consequently, a given temperature increase

enhances longwave radiation in the cold Arctic less than it does in the tropics, for example. Since increased emission of longwave radiation counteracts warming, this is another effect contributing to Arctic amplification (Pithan and Mauritsen, 2014).

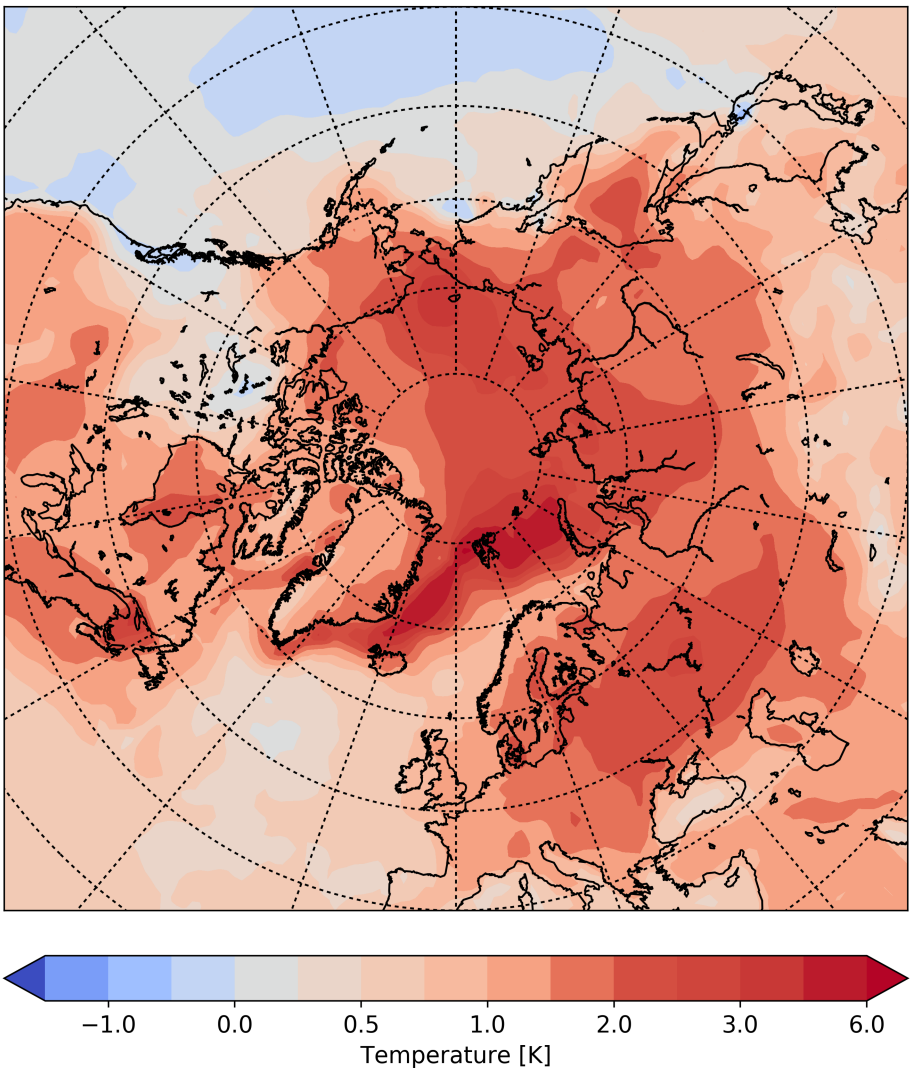

Figure 2.3: Difference of mean surface temperature between the periods 2001-2010 and 1961-1970 based on the ERA-20C atmospheric reanalysis. Positive values denote a temperature increase.

It is clear that the above-average Arctic warming reduces the temperature gradient between mid-latitudes and polar regions and increases the geopotential height of pressure surfaces in the Arctic. The effects of Arctic amplification and sea ice loss on mid-latitude weather patterns have been heavily debated in the last few years, but due to the complex interactions,

nonlinear mechanisms and high internal variability of the mid-latitude and Arctic climate system there is no consensus on specific consequences yet. To provide an example, a well-established hypothesis links the reduced baroclinity to more persistent weather patterns in the mid-latitudes, potentially promoting an increase of droughts and flooding events (Screen and Simmonds, 2014). However, more observations and longer time series are necessary to assess whether Arctic amplification already had impacts on mid-latitude weather and to unequivocally detect cause and effect (Overland et al., 2016).

Significant Arctic warming is expected to continue throughout the rest of the century, although the magnitude of future Arctic amplification is rather uncertain as climate model projections differ significantly in terms of feedback responses. Based on current Earth system models, mean Arctic warming until the end of the century could be 2.2 to 2.4 times higher than the global average, corresponding to a temperature increase of approximately 4 °C to 8 °C (scenarios RCP4.5 to RCP8.5) between 2081-2100 compared to 1986-2005 (IPCC, 2013). As observed today, warming in early winter and over the Arctic ocean will likely be most pronounced, while the temperature increase in summer is smaller. Rising precipitation trends due to enhanced local surface evaporation and poleward moisture transport are also very likely (Bintanja and Selten, 2014). Climate models simulate a precipitation increase of 15 % to 50 % compared to the period 1986-2005 until the end of this century, but uncertainty is relatively high (IPCC, 2013).

The implications of climate change for terrestrial ecosystems in Arctic tundra are heavily debated due to complex interactions between atmosphere, hydrology, soil and vegetation (see Fig. 2.4). The large carbon pool in Arctic ecosystems has received widespread scientific attention, as parts of it could be released to the atmosphere as greenhouse gases, providing a potentially significant feedback process in a magnitude of global importance. At the same time, atmospheric warming causes a shift of vegetation zones towards the poles, and stimulates plant production in Arctic tundra. By this mechanism, large amounts of carbon could be sequestered in biomass, considering that plant growth is currently strongly limited and vegetation carbon stocks are very low.

2.3.1 Permafrost carbon feedback

Permafrost thawing makes large amounts of organic carbon, which have been sequestered for thousands of years, available for microbial decomposition, subsequently leading to a release of greenhouse gases to the atmosphere. This is one of the most well-known terrestrial

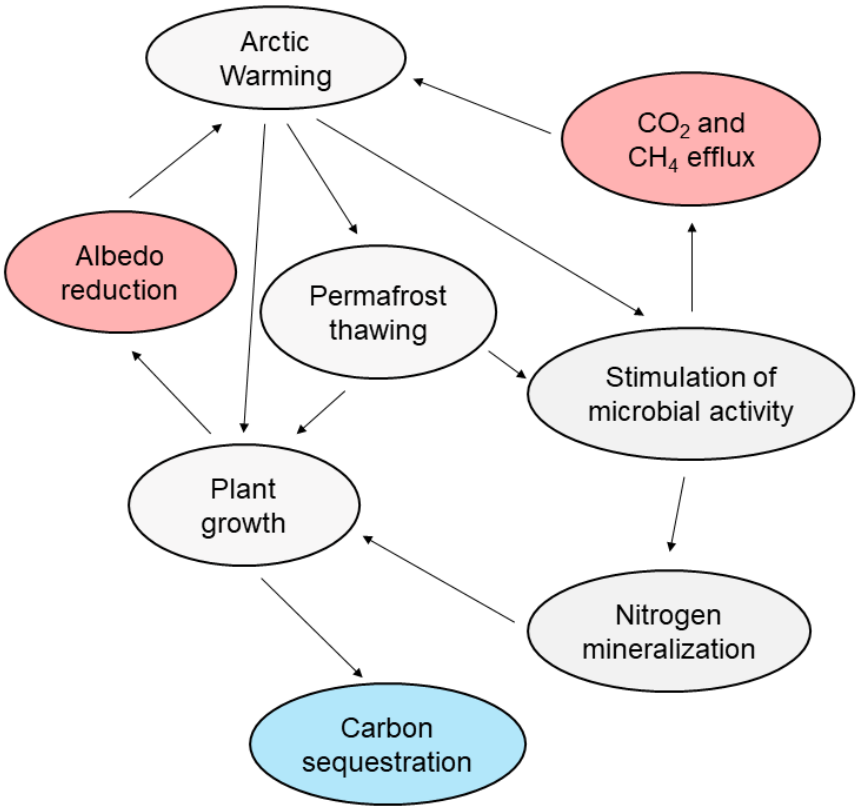

Figure 2.4: Simplified overview of high-latitude ecosystem processes triggered by climate change. Positive feedbacks to warming are depicted in red, negative feedbacks in blue.

feedback processes of climate change in high latitudes, yet the amount and timing of greenhouse gas release are still relatively unclear. The fact that carbon can be released in form of carbon dioxide or methane, depending on oxygen availability in the soil, further complicates projections. Knowledge of the proportion is critical, as methane is a much more potent greenhouse gas than CO_2, having a global warming potential (GWP) of 34 when considering a time horizon of 100 years and including climate-carbon feedbacks (IPCC, 2013).

Upon thawing, incubation experiments suggest rapid decomposition of the most labile carbon – independent of its age – followed by a decline of carbon degradation (Knoblauch et al., 2013). Rates of decomposition and carbon loss vary widely among permafrost soils; in aerobic environments those variations can be largely attributed to the carbon to nitrogen ratio, with higher values indicating higher emissions (Schuur et al., 2015). Hotspots of greenhouse gas releases are therefore to be expected in places where permafrost thaw exposes

carbon reservoirs that are big and easily decomposable, i.e. where substantial amounts of organic carbon are present.

Some permafrost soils contain considerable amounts of ice. Seasonal or permanent melting of this ice causes subsidence of the surface and leads to a characteristic, uneven topography referred to as thermokarst, in analogy to similar-looking karst landscapes, although the formation mechanisms are entirely different. When water pools develop in poorly drained soils of the subsidence areas, thermal conductivity rises, contributing to further thaw of the underlying permafrost. By this process, tens of metres of permafrost can thaw within just a couple of years. In contrast to common, gradual top-down thawing, the abrupt thawing associated with thermokarst occurs only at point locations, but it potentially transforms entire regions into mosaics of wetlands. There is increasing evidence that large parts of lowland tundra are vulnerable to thermokarst development (Grosse et al., 2013; Schuur et al., 2015). On a local scale, abrupt thaw events with subsequent freezing have frequently occurred since the last Ice Age, but climate change will likely trigger this process in many tundra lowland ecosystems, leading to further expansion of thermokarst landscapes. Observations already document an increase of lake area since the 1970s in some northern ecosystems, for example in northwestern Canada and in Alaska (Baltzer et al., 2014; Raynolds et al., 2014).

The waterlogged, anaerobic soils in parts of thermokarst landscapes, and in wetlands in general, strongly influence decomposition processes: Some of the highest methane emissions in Arctic tundra were observed in thermokarst thaw lakes (Olefeldt et al., 2013). However, permafrost soil incubation experiments show that cumulative carbon emissions over one year are on average 78 % to 85 % lower in anaerobic soils compared to aerobic soils (Schuur et al., 2015). Considering the contribution to climate change, the effects of reduced carbon emissions are partially offset by the higher GWP of methane (see Fig. 2.5). Still, experiments suggest that decomposition of recently thawed permafrost soils contributes more strongly to climate change if the soils are dry, highlighting the control soil hydrology exerts. Additionally, laboratory experiments do not account for potential oxidation of methane in aerobic soils above the water table, which would further reduce the climate impact of methane production in deeper anaerobic soils. If thermokarst landscapes and peatlands were drained, for example during drought periods, the lowered water table and oxygenation of soils would lead to increased carbon emissions (Schuur et al., 2015).

Current Earth system models, which already include most permafrost-specific processes identified to be of major importance, project cumulated carbon emissions from degrading permafrost under the pessimistic RCP8.5 scenario in the range 37 PgC to 174 PgC by 2100, with an average of (92 ± 17) PgC. However, Earth system models underestimate today's

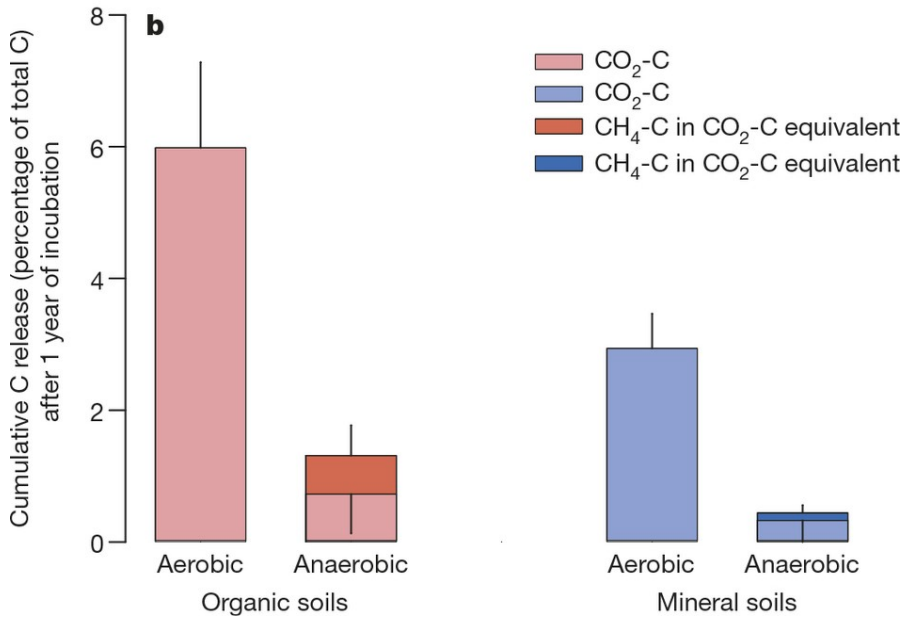

Figure 2.5: Incubation experiments of permafrost soils showing carbon losses, cumulated over one year, under aerobic and anaerobic conditions for organic soils ($> 20\% C$, $N_{aerobic} = 43$, $N_{anaerobic} = 28$) and mineral soils ($< 20\% C$, $N_{aerobic} = 78$, $N_{anaerobic} = 25$), measured at 5 °C. Darker colours indicate the CO_2 equivalent on a hundred year timescale based on reference values from IPCC (2013), error bars delimit upper and lower 97.5 % confidence interval. Adapted from Schuur et al. (2015).

permafrost carbon pool, because most of them consider carbon only down to 3 m depth, potentially restraining modelled carbon release. Therefore, the fraction of their initial permafrost carbon pool subsequently lost to the atmosphere is a more meaningful quantity: Across models, this value is relatively constant with (15 ± 3) % until 2100. An expert assessment based on these dynamic models and other approaches such as laboratory experiments came to the conclusion that around 5 % to 15 % of the present permafrost carbon pool are vulnerable to loss until 2100; with 10 % being equivalent to 130 PgC to 160 PgC (Schuur et al., 2013). If emitted at a constant rate, greenhouse gas emissions from degrading permafrost would be comparable to emissions by land-use change, but far lower than anthropogenic fossil fuel emissions. A rapid pulse of permafrost thawing and subsequent greenhouse gas release would have more severe consequences, but at the moment, there are no indications for such an event. Instead, long-term simulations indicate continuing relevance of permafrost carbon feedback in the following centuries and project that 59 % of total permafrost carbon release will occur after 2100, although uncertainty is substantial. Not all Earth system models discriminate between CO_2 and CH_4 emissions, but in the expert assessment conducted by Schuur et al. (2013) future methane emissions around 2 % to 3 % of total carbon emissions

in permafrost regions were expected.

Uncertainties are largely associated with abrupt thawing, because it is not part of current large-scale models, which simulate a gradual warming of permafrost soils. To address the implications of abrupt thawing and thermokarst formation, detailed modelling of soil thermal regime and hydrology as well as further research efforts to clarify the relative importance of abrupt thawing compared to gradual thawing will be necessary.

2.3.2 Stimulation of plant growth and decomposition

Rising air temperatures and precipitation sums, lengthening of the growing season, elevated levels of atmospheric CO_2 and increased nutrient release from decomposing organic matter will stimulate primary production and carbon sequestration in plant biomass in large parts of high northern latitudes in the course of climate change. Coinciding with increasing temperatures in the past few decades, an overall trend of greening, increasing productivity and shrub expansion is already observed, albeit with regional variations (Goetz et al., 2005).

The temperature increase, enhanced productivity and northward shift of vegetation zones contribute to several positive and negative feedback processes between biosphere and atmosphere: Expansion of shrubs and trees decreases the albedo of land surface (also during the winter by masking the snow cover), thus increasing absorption of short-wave radiation and sensible heat flux to the atmosphere (Beringer et al., 2005); higher evapotranspiration rates due to increased plant biomass and larger leaf area remove latent heat at the surface, but increase atmospheric water vapour content and enhance absorption of long-wave radiation; shading by canopy reduces ground heat flux, soil temperature and thus also soil respiration; warming stimulates microbial decomposition, releasing greenhouse gases, but also increasing nutrient mineralization.

Statistical and process-based models indicate that large parts of Arctic tundra – likely more than 50 % – will be affected by vegetation shifts until 2050, and aboveground plant biomass will increase by 15 % to 68 % (Pearson et al., 2013). Until the end of the century, NPP north of 60°N could increase by 80 % (Qian et al., 2010). Pearson et al. (2013) also report that the decrease of albedo will likely be large enough to offset a potential reduction of soil temperature by shading.

Higher soil temperatures stimulate microbial activity and thereby increase nutrient mineralization in the soil. This will favour plant production and the expansion of shrubs, since many tundra regions are currently limited by nutrient availability. In a long-term fertilization

experiment in Alaskan tundra, aboveground carbon storage and productivity increased, but in total, carbon was lost from the ecosystem, due to accelerated decomposition of deep, older carbon stored in the soil, which may have been caused by direct nutrient stimulation of decomposition or by indirect effects like the shift of microbial community composition (Mack et al., 2004). In any case, increased decomposition and subsequent release of older soil organic carbon could offset the carbon accumulation by new plant biomass in some Arctic environments.

In partly water-limited polar deserts and semi-deserts of the high Arctic, changes in precipitation patterns and soil moisture regimes could also contribute to shifts of vegetation distribution. In field experiments conducted in northwestern Greenland, combined warming and wetting treatment strongly increased net ecosystem production, whereas warming treatment alone caused a stronger increase of ecosystem respiration relative to gross primary production. Furthermore, more deep, old carbon was lost without wetting (Lupascu et al., 2014).

It is still greatly uncertain, how the opposing consequences of climate change – stimulation of carbon sequestration in biomass, and enhancement of microbial decomposition – will affect the future carbon balance of Arctic tundra. Current Earth system models simulate that land carbon uptake exceeds release of carbon to the atmosphere in the following decades, but eventually, the capacity of vegetation to sequester carbon is surpassed by carbon release from microbial decomposition (Schuur et al., 2015). While rising atmospheric CO_2 concentrations are expected to promote plant growth in all ecosystems around the world, Arctic tundra could be one of the few regions, where temperature and precipitation changes would favour land carbon uptake, at least in the short term (IPCC, 2013). On a global scale, the sign and magnitude of future land carbon storage are highly uncertain, although multi-model averages of the latest Coupled Model Intercomparison Project (CMIP5) indicate a small land carbon sink.

3 Effects of experimental warming on soil respiration in a polar semi-desert

In order to assess climate change effects on soil respiration in high latitudes, data of a controlled warming experiment in Svalbard was evaluated. In this chapter, background information on the experiment will be given, and methodology and results will be described and discussed.

3.1 Introduction

Understanding and quantifying the terrestrial feedback to climate change is essential for projecting the future of our environment. Effects of climate change are particularly severe in Arctic tundra, but timing and magnitude of feedback processes are relatively uncertain, yet possibly of high relevance. The experiment described in this chapter aims to clarify the trend of an important component of the carbon cycle – soil respiration – in one of the regions that already underwent dramatic warming in recent decades and years, a polar semi-desert in the far north. The objective is to address the following questions: How is soil respiration affected by rising temperatures? Are there seasonal differences of the warming effects? Furthermore, does the temperature sensitivity (Q_{10}) of soil respiration change with warming? How do precipitation and wind speed affect soil CO_2 efflux at high latitudes?

3.2 Study site

Located in the high Arctic between 74°N to 81°N and 10°E to 35°E, Svalbard is one of the world's northernmost continuously inhabited archipelagos. It consists of more than 400 islands, the largest being Spitsbergen, followed by Nordaustlandet, Edgeøya and Barentsøya, with permanent human settlements only on the main island of Spitsbergen. Svalbard's land

Month	J	F	M	A	M	J	J	A	S	O	N	D	Annual
T [°C]	-11.7	-12.9	-12.6	-9.6	-2.6	3.3	6.6	5.8	1.6	-4.6	-7.8	-10.5	-4.6
RR [mm]	18	15	18	10	7	9	18	22	23	16	19	21	195

Table 3.1: Average monthly temperatures and precipitation sums at Longyearbyen airport in the period 1986-2015.

area adds up to 61 022 km^2, of which about 60 % is permanently covered with ice and snow, and only 10 % is covered with vegetation (Elberling, 2007).

For the following evaluation of Svalbard's climate and its recent changes, weather data recorded in Longyearbyen, the largest town and administrative centre of Svalbard, was used. The weather station (WMO code 01008), operated by MET Norway, is situated at the airport, 4 km northwest of the town centre, at an altitude of 27 m. Weather observations in Svalbard have a long history and reach back to 1911, but the weather station was relocated several times, the last time in 1975, when the new airport was opened (Førland et al., 2012). Although a homogenised temperature time series since the early twentieth century exists, only data from the current location at the airport was taken into consideration to rule out homogenisation errors.

Based on the classification by Köppen and Geiger, Svalbard belongs to the polar climate zone that is mainly characterised by the lack of warm summers, implying that maximum monthly average temperature is lower than 10 °C (see section 2.2). Nevertheless, considering the high latitude and the proximity to the North Pole, the climate is surprisingly mild, because it is tempered by the warm West Spitsbergen Current, a branch of the North Atlantic Current. The warm current also causes that the eastern part of the Greenland sea, situated directly west of Spitsbergen, is largely ice free, even during winter. Still, the climate is too cold to support tree growth and larger vegetation. July and August are typically the warmest months with average temperatures between 5 °C to 7 °C, while lowest monthly mean temperatures of −13 °C to −7 °C (see Tab. 3.1) occur relatively late in winter, in February and March, after the long polar night, which lasts from 27 October until 14 February. By contrast, the midnight sun is visible from 19 April to 23 August.

In the 10-year period between 2006 and 2015, the mean annual air temperature in Longyearbyen was −2.9 °C, compared to −6.3 °C between 1976 and 1985. This drastic increase – a rate of approximately 1 °C per decade – illustrates the substantial climate warming documented in most parts of the high Arctic (IPCC, 2013) and makes Svalbard one of the world's areas with the fastest observed temperature increase due to climate change (compare Fig. 2.3 in

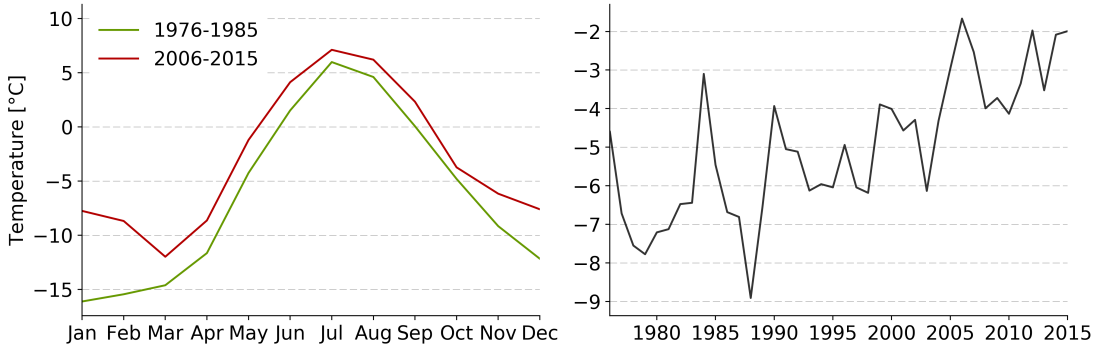

Figure 3.1: Comparison of monthly average temperatures at Longyearbyen airport between the periods 1976-1985 and 2006-2015 (left side). On the right side, the time series of annual mean temperatures at Longyearbyen airport since 1976 is shown.

section 2.3). The warming is more pronounced in winter, as the mean air temperature in January has risen from −16.1 °C between 1976 and 1985 to −7.8 °C between 2006 and 2015, whereas the temperature in July has risen by 1.4 °C comparing the same periods (see Fig. 3.1). The warming trend is observed since the late 1960s; while the temperature increase until the 1990s can be largely attributed to changes in the atmospheric circulation, which promoted warm, southwesterly and southerly winds in Svalbard, the warming in the past 20 years shows different patterns and is likely caused by the direct and indirect effects of sea ice loss (Overland et al., 2011; Førland et al., 2012).

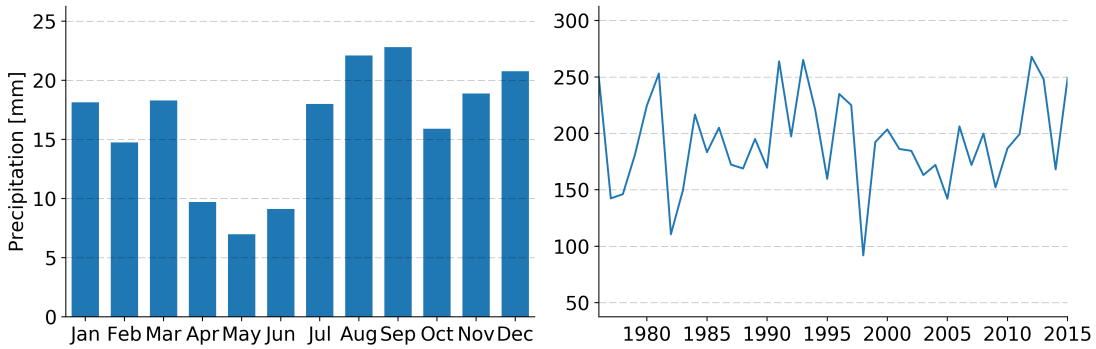

Figure 3.2: Average monthly precipitation sums in the period 1986-2015 (left side) and time series of annual precipitation at Longyearbyen airport in the past 30 years (right side).

Considering annual precipitation, no significant trend in recent decades can be found (see Fig. 3.2), although rising temperatures and sea ice loss would suggest increased evaporation. Since measurements at Longyearbyen airport began, the average annual precipitation sum of each decade is approximately 195 mm. Highest monthly precipitation is observed in late

summer and during the winter with roughly 20 mm per month, and lowest precipitation amounts are documented in spring, reflecting typical pressure patterns of Arctic and subarctic areas. The lowest annual precipitation sum during the last 40 years was 92 mm, observed in 1998, and the highest was 310 mm, recorded in 2016.

The soil CO_2 efflux measurement site is also located close to Longyearbyen, 5 km southeast of the town centre at 78.187°N and 15.762°E in the polar semi-desert ecosystem of Endalen valley. The measurement devices are placed on a well-drained slope at an altitude of 40 m above sea level (see Fig. 3.3).

Figure 3.3: Measurement site seen from the valley floor of Endalen.

The organic soil layer in Endalen is very thin and characterised by weak soil development. It contains significant amounts of talus material that accumulated from the bare rock above the observation site. Due to its shallow depth, typically the whole organic layer thaws during the summer, so the pool of organic carbon stored in permafrost is negligible. The vegetation cover – comprising dwarf shrubs, herbs and mosses, and being dominated by Dryas – is sparse as well, contributing to the small carbon storage in this ecosystem.

Since 2001, the site in Endalen is one of the locations of the International Tundra Experiment (ITEX), a research network aiming to understand the long-term consequences of climate change for vegetation and biogeochemical processes in high latitudes (Henry and Molau, 1997). As part of the experiment, some plots on the slope are artificially warmed using so-called open-top chambers (see section 3.3.1), and as a result of the long runtime, increases

in vegetation cover and plant biomass in warmed plots are clearly visible.

3.3 Materials and methods

3.3.1 Open-top chambers

For simulating additional warming, so-called open-top chambers (OTCs) were used in this experiment (see Fig. 3.4). They became a standard method for microclimate manipulation in tundra and alpine sites in the 1990s, during the early history of the ITEX project (Marion et al., 1997). There are different OTC designs varying in shape, size and material; the OTCs in Endalen consist of hexagonally arranged, translucent fibreglass walls, inclined towards the inside by approximately 60° with respect to the horizontal. While shortwave, solar radiation is transmitted through the fibreglass, outgoing, terrestrial longwave radiation is partly trapped, causing an increase of incoming net radiation and raising surface and soil temperature. The mean soil temperature increase induced by OTCs is often cited to be 1 K to 2 K based on the findings of Marion et al., but a more comprehensive study by Bokhorst et al. (2013) found average annual temperature increases of approximately 0.8 K with relatively little variation across several locations in polar and alpine regions – equally for close-surface air (10 cm to 15 cm above ground), surface and soil temperature. Generally, they observed that summer and winter temperatures increased most – 0.9 K to 1 K – and autumn and spring temperatures were enhanced a little less, by 0.5 K to 0.6 K, although seasonal temperature increases – in contrast to the annual temperature effect – varied considerably across different sites. In the summertime, the temperature effect correlates strongly with solar irradiance, and therefore, the increase is most pronounced in the daytime. During winter, trapping of snow inside the OTCs and the subsequent increase of snow depth and better soil insulation are the main drivers of OTC warming. Moreover, the frequency of extreme low-temperature events is reduced, while high temperatures are observed more often. As a result of higher temperatures, evaporation from OTC sites tends to be enhanced, but this effect is partly offset by the retention of snow in winter and spring. In the study of Bokhorst et al., soil moisture in warmed plots was slightly lower than in control plots, but the difference was not significant.

Furthermore, the vegetation enclosed in the OTCs may affect the temperature increase as well. In Endalen, Bokhorst et al. identified higher OTC temperature increases in plots with sparser vegetation, probably because denser plant cover more effectively shields the soil

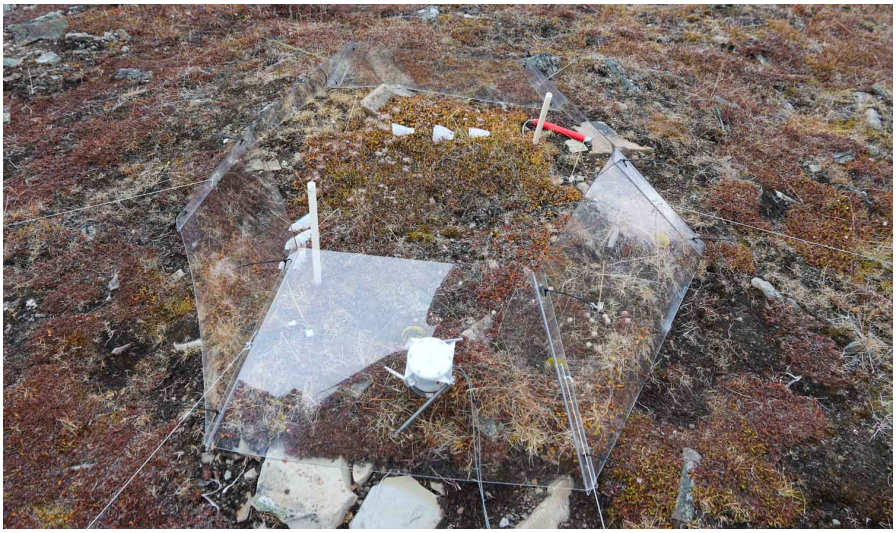

Figure 3.4: A passive open-top chamber in the field.

from incoming solar radiation and the OTCs therefore trap heat less efficiently. Other microclimatic effects of OTCs, for example the reduction of wind speed, are less well-documented, but seem to vary across sites. Wind speed reduction could contribute to create a more favourable environment for vegetation enclosed in the OTCs (Marion et al., 1997).

While OTCs passively warm the enclosed plot, other experiments rely on active warming methods, which involve soil heating elements, such as electrical heating cables and fluid heating pipes, or infrared heaters. The main advantage of active designs is the capability to precisely control timing and magnitude of temperature increase; passive designs on the other hand are inexpensive, reliable, easy to deploy, do not require power supply and do not disturb the soil. Conversely, one of the disadvantages of OTCs is the rather variable effect on temperature. Furthermore, OTCs alter the local soil hydrology (mainly by snow retention) and reduce near-surface wind speed, potentially affecting soil CO_2 efflux.

3.3.2 Soil carbon dioxide efflux measurements

For measuring the soil CO_2 efflux rate, passive, forced-diffusion (FD) dynamic chambers as described by Risk et al. (2011) were used. As depicted in Fig. 3.5, they consist of several components. A small PVC cylinder with an internal diameter of 5 cm and a height of 8 cm acts as embodiment. It is attached to the ground using a soil collar with legs, providing a gas seal and support in the ground. A Vaisala GMP343 CO_2 sensor is placed into the embodiment for measuring the CO_2 molar concentration within the chamber, subsequently denoted

as C_{chamb}. The bottom of the chamber is covered with a gas-permeable and hydrophobic membrane to allow gas flow from the soil into the chamber, but protect it from water and ice. Additional openings on the side of the device, also covered with gas-permeable membranes, connect the chamber headspace with the atmosphere, and establish equilibrium mixing between atmospheric CO_2 and soil CO_2 moving into the chamber. Therefore, solely free air diffusion and thermal convection act as mixing agents. For the calculation of the soil CO_2 efflux rate, the atmospheric molar concentration of CO_2, C_{atm} must be quantified as well. It is measured in a chamber identical to the one described above, except for the bottom membrane being replaced by a thick rubber piece to prohibit gas exchange with the soil, so the only openings are the membranes on the side of the chamber. Fig. 3.6 shows a FD chamber in the field.

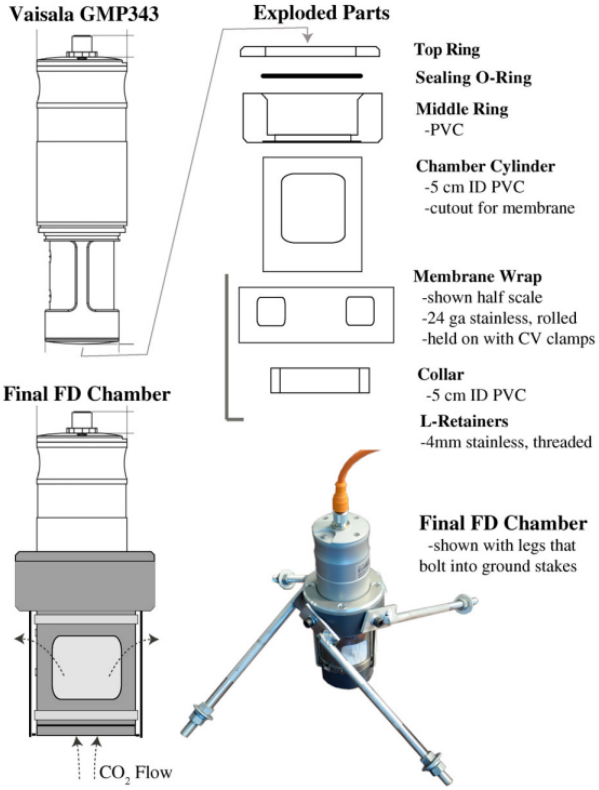

Figure 3.5: Schematic of the FD chamber type used for the measurements. Adapted from Risk et al. (2011).

The relationship of the molar concentrations of CO_2 in the chamber and the atmosphere is described by the following equation:

$$V\frac{\partial C_{chamb}}{\partial t} = A_s R(t) - A_a\left(D\frac{C_{chamb}-C_{atm}}{L}\right) \tag{3.1}$$

Here, V [m^3] is the chamber volume, A_s [m^2] is the area of the chamber in contact with the soil, $R(t)$ [$\mu mol\, m^{-2}\, s^{-1}$] is the time-dependent flux rate, A_a [m^2] is the membrane area in contact with the atmosphere, D [$m^2\, s^{-1}$] is the diffusivity through the chamber volume and across the membranes, L [m] is the characteristic path length for diffusion, and, as described above, C [$\mu mol\, m^{-3}$] is the molar concentration of CO_2. The equation is the mathematical expression for the trivial statement that the temporal change of CO_2 concentration in the chamber equals incoming minus exhausting soil gas. Considering that C_{chamb} changes very slowly with time in most measurement environments, the left-hand side of the equation can be neglected compared to the bigger terms on the right-hand side. As a consequence, the equation can be rearranged:

$$R_s = \frac{A_a}{A_s}\left(D\frac{C_{chamb}-C_{atm}}{L}\right) \tag{3.2}$$

In this case, the substitution $R_s = R(t)$ is valid, because the time-dependency of C_{chamb} was neglected. Except for the CO_2 concentrations, only constants related to the chamber design and membrane material are left on the right-hand side, making this equation suitable for determining the efflux rate, when CO_2 concentrations are measured and the constants are known. In practice, the constants are grouped together in a single chamber constant, $G = \frac{A_a D}{A_s L}$ [$m\, s^{-1}$]. G is established by calibration and can be manipulated by using different membrane sizes and materials.

$$R_s = G\,(C_{chamb} - C_{atm}) \tag{3.3}$$

Under normal atmospheric, geological and biological conditions, C_{chamb} will always be greater than C_{atm}, indicating positive CO_2 flux rates directed from the soil to the atmosphere. The larger the difference between chamber headspace and atmospheric CO_2 concentrations, the more precise the results of this method are. As C_{chamb} itself depends not only on the soil efflux, but also on properties of the chamber, a higher measurement accuracy can be achieved by appropriate design. However, with increasing values of C_{chamb}, the issue of lateral diffusion arises. High CO_2 concentrations in the chamber reduce the concentration gradient at the soil surface, thus decreasing the soil CO_2 efflux into the chamber by favouring a lateral flow within the soil, away from the chamber, eventually causing an under-reporting

of flux rates. Therefore, there is an inevitable trade-off between measurement accuracy and the lateral diffusion problem. The underestimation can be particularly pronounced during periods of high atmospheric diffusivity, for instance caused by high wind speeds, and in dry, high-diffusivity soils. The inverse case, overestimation of true flux rates by lateral diffusion, is also possible when the ground is covered with snow, which leads to a decrease in diffusivity above the soil surface, causing a channelling of soil gases through the chamber. As a consequence, data obtained during snow cover periods has to be treated cautiously.

Another potential source of error is the pressure gradient that may be established between chamber headspace and atmosphere, caused by high wind speeds, warming or cooling of air inside the device or by circulating gases (Davidson et al., 2002). In order to accommodate pressure changes and to prevent the effect, this chamber design relies on venting by the membranes. Since they are relatively large compared to the volume of air inside, the measurement error caused by this effect should be negligible.

Figure 3.6: One of the FD chambers during field use in Endalen. The two cables on the left-hand side are leading to the power supply and data logger. Below the cables, one of the four membranes is visible.

The exact location of the chamber must be chosen carefully, as soil effluxes may vary considerably over a small area. Consequently, using several devices is beneficial. Also, plant material enclosed in the chamber may influence C_{atm} as it decomposes, thereby releasing CO_2. On account of this, placing the FD chambers on heavily vegetated surfaces should be avoided. Furthermore, the chambers have to be fixed tightly to the ground, so CO_2 cannot

leak through other openings than the membranes, and the inside of the chamber is not exposed to light. Furthermore, C_{atm} and C_{chamb} should be measured close to each other, because the molar concentration of carbon dioxide in the atmosphere varies both vertically and laterally; especially close to the surface, despite the fact that it is a relatively well-mixed trace gas in general.

In contrast to this relatively new FD chamber design, older designs maintain equilibrium between atmosphere and soil gases by using pumps rather than by diffusion through membranes. The passive design results in lower maintenance costs and energy consumption, making the device more suitable for longer field experiments, and allowing measurements with relatively high frequency. However, especially when working with long-time datasets, a possible drift of the chamber constant G has to be considered, as the gas-permeable membranes are degraded by UV radiation, particle abrasion and possibly biofouling. Nevertheless, Risk et al. found only little variation of G over the course of a few months, and recommend membrane replacement intervals between "several months to one year, depending on the environment".

3.3.3 Experimental design and data analysis

In total, six FD dynamic chambers were used to measure soil CO_2 efflux rate every 4 hours: Data was logged at 0, 4, 8, 12, 16 and 20 Central European Time (CET). Three chambers were placed in different OTCs and three more chambers placed on separate plots outside of the OTCs served as control measurements. All devices were located relatively close to each other, within a radius of approximately 10 m (see Fig. 3.7). An additional chamber between experimental warming and control plots was used to measure C_{atm}. A battery loaded by a photovoltaic module was used as a power supply. However, the logging interval turned out to be too short to sustain power supply during winter, which caused logging of soil respiration data to stop on 17 October 2015, thereby losing information about soil respiration in winter. Logging restarted on 6 April 2016, and continued until data was read out on 4 October 2016.

Before applying more sophisticated methods, obviously erroneous, negative flux rates were marked as invalid. Thereby, already 1178 of in total 10152 values were excluded. Afterwards, a similar procedure to the one described by Savage et al. (2008), adapted for the low CO_2 fluxes expected in this ecosystem, was used for eliminating other suspect soil respiration values, which was possible since measurements were carried out in a relatively high frequency (compared with traditional methods of soil respiration measurements). Each CO_2 efflux value of a chamber was compared to the mean of the other warming or control chambers,

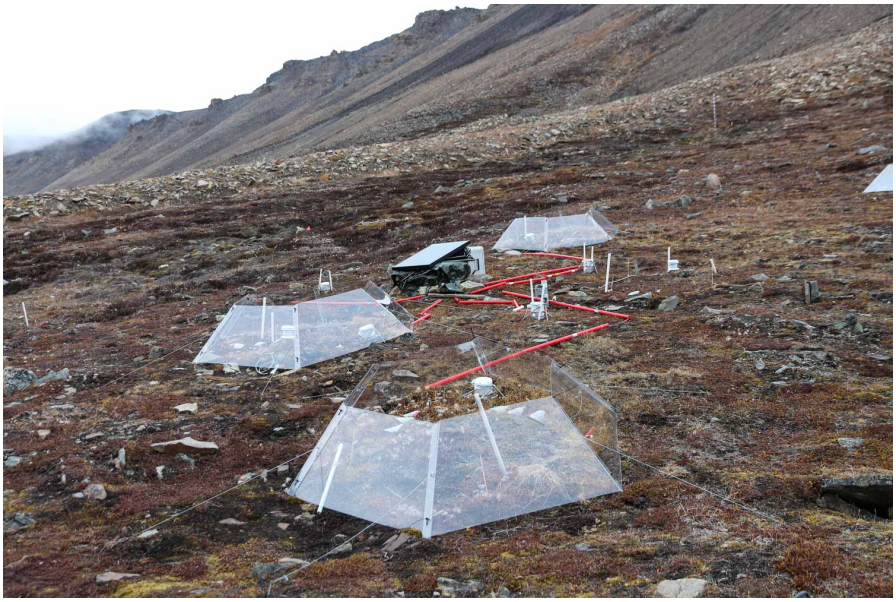

Figure 3.7: Setup of the experiment: The three FD chambers placed in OTCs as well as the FD chambers of the control plots can be seen. The red tubes, used as protection against animals, contain cables leading to the data logger and the power supply.

respectively. If the ratio of individual efflux value to the mean of the other chambers was < 0.5 or > 2, this value was marked for further investigation. Then, the suspicious value was tested for temporal consistency: If it differed by more than $0.2\,\mu\text{mol}\,\text{m}^{-2}\,\text{s}^{-1}$ from both the preceding and subsequent value, the value was eliminated, otherwise it was kept. Data from one of the control chambers had to be excluded for the entire measurement period, because it was hardly correlated with other plots and didn't vary with temperature. Overall, including the elimination of negative values, 2562 of 10152 values were considered invalid.

To analyse systematic differences of soil respiration between warmed and control sites, daily averages of efflux data across the three warmed plots and the two remaining control plots were computed, and a Welch t-test was performed to examine the significance of potential differences. Moreover, data from the weather station at Longyearbyen airport (see section 3.2), located about 9 km away from the measurement site in Endalen, was used to gain information about the environmental conditions that prevailed during the measurements. Air temperature, precipitation and wind speed were compared to the flux measurements to analyse their relative importance as controls. Daily average temperatures, which were calculated as arithmetic mean of hourly air temperature measurements, and daily average efflux rates were used to calculate Q_{10} values for warming and control plots based on a simple first-order exponential relationship (see section 2.1.2). In contrast to precipitation and wind

speed data, which had no gaps, in total three weeks of temperature data were missing: One week around the beginning of August 2015 and two weeks in late April and early May 2016.

3.4 Results

3.4.1 Temperature and precipitation

Daily average temperatures on days with valid efflux measurements (i.e., excluding the period between 17 October 2015 and 6 April 2016) ranged from −13.5 °C, observed on 11 April 2016, to 12.1 °C on 2 July 2016. The lowest daily average temperature in the winter 2015/16 was −16.8 °C, measured on 13 December 2015, when the FD chambers were without power supply. Daily means of almost every day during the measurement campaign were higher compared to the official climate normal period from 1961 to 1990, illustrating the increasing temperature trend in recent decades. The anomalies were most pronounced in autumn and winter, while they were relatively small in summer. August 2016, for example, was only 1.1 K warmer than the long-term average, while temperature anomalies both during the winter 2015/16 and at the end of the measurements in autumn 2016 were striking, as new records were set across the entire Arctic. In January 2016, the mean temperature in Longyearbyen was −3.8 °C, 11.5 K above the climate normal, and in October 2016, the average temperature was 8.7 K higher than average, surpassing the previous October record by 1.8 K. Even when referring to average monthly temperatures between 2006 and 2015 instead of the climate normal period, every month with the exception of August 2016 was warmer than the mean in that reference period.

Flux measurements began after a relatively dry period in spring and early summer 2015. In five consecutive months, from March to July, negative precipitation anomalies were observed, with 50 % less precipitation than on the long-term average. Starting from mid-August, however, rainfall increased, and the second half of the year was wetter than on average. First snowfall events occurred in early October, and a thin, but continuous snow cover was reported on 13 October, already after logging had stopped. Except for short breaks in November, a snow cover remained for the rest of the winter, with a maximum snow depth of 14 cm in the beginning of April. The last day with a snow cover at Longyearbyen airport was 9 May, but it is likely that snow melted some days earlier on the exposed south-east facing slope in Endalen. After the wet period from August to January, another dry period between February and June 2016 was observed, with 65 % less precipitation than in the reference period of the climate normal. Similar to the year before, the trend reversed in

summer, although this time, above-average rainfall was already encountered in July. Until the end of the year, every consecutive month had unusually high precipitation, turning the precipitation balance far above average: Accumulated over the year, a new record was set with 310 mm, about 50 mm more than the previous record.

3.4.2 Soil respiration

Relative to other ecosystems, observed soil respiration rates in Endalen were very low, highlighting the low productivity and carbon turnover in polar semi-deserts. Temporally, efflux rates across all plots were generally highest and most variable in summer, when microbial activity was stimulated by favourable soil temperatures and exudations of plant roots, whereas efflux was lower and relatively constant in autumn, when solar irradiance diminished and variation of soil temperature was restricted. Furthermore, low rates and little variation were documented in April, when the surface was still covered with snow.

Over the course of the experiment, soil respiration in warmed plots was significantly enhanced relative to control plots ($P > 0.99$). The daily average soil CO_2 efflux rate in experimentally warmed plots was $(0.23 \pm 0.12)\,\mu mol\,m^{-2}\,s^{-1}$, compared to $(0.14 \pm 0.11)\,\mu mol\,m^{-2}\,s^{-1}$ in control plots. Particularly in late summer and autumn, warmed plots had considerably higher soil respiration rates, while CO_2 efflux from control plots even exceeded efflux from warmed plots in some days in spring and early summer (see Fig. 3.8). During one day around snow melt in early May, the average efflux rate of control plots was three times larger compared to warmed plots, probably the result of freeze-thaw cycles or the release of soil CO_2 that accumulated below the snow cover.

Effluxes from all plots (except for the excluded control chamber) showed a clear temperature response and increased with temperature. The correlation coefficients R^2 for warmed and control plots were 0.54 and 0.44, respectively. Regarding differences in their temperature sensitivity, warmed plots had considerably enhanced respiration at all temperatures, but in particular below freezing point. For $T < 0\,°C$, efflux from warmed plots, averaged over all measurements meeting this condition, was 2.17 times higher (0.124 vs. $0.057\,\mu mol\,m^{-2}\,s^{-1}$) than efflux from control plots, whereas the ratio was 1.52 (0.299 vs. $0.196\,\mu mol\,m^{-2}\,s^{-1}$) when considering only days with $T > 5\,°C$. This effect is also mirrored in the Q_{10} of warmed and control plots: First-order exponential fitting resulted in a Q_{10} of 1.9 of experimentally warmed plots and 2.2 of control plots, i.e. the temperature sensitivity of control plots was slightly higher (see Fig. 3.9).

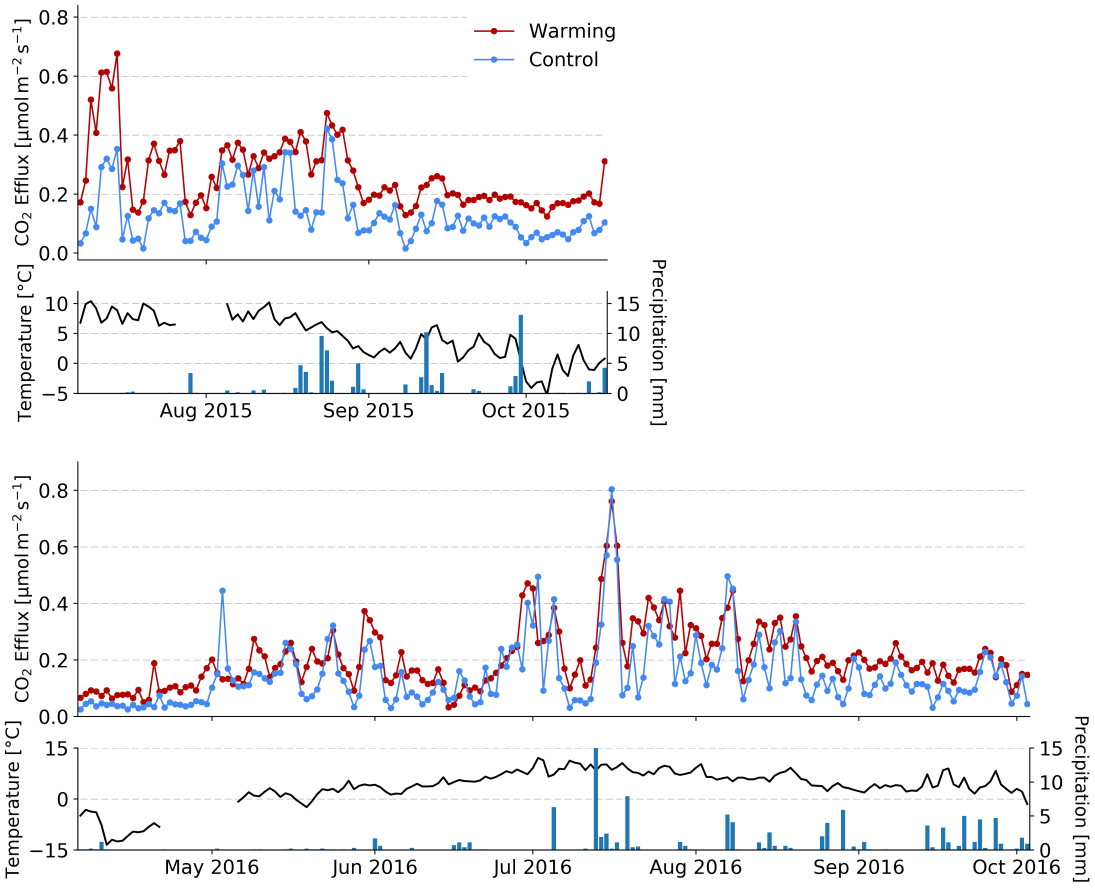

Figure 3.8: Daily averages of soil CO_2 efflux rates as measured in warmed (red line) and control (blue line) plots between 8 July 2015 and 16 October 2015 (upper plot) and between 6 April 2016 and 3 October 2016 (lower plot). Additionally, daily average air temperatures (black line) and precipitation sums (blue bars) at Longyearbyen airport are depicted.

Soil respiration tended to increase after precipitation events, mediated by soil water content. Highest efflux in 2016, for example, was observed in mid-July shortly after the major rainfall event during the growing season. However, the effects of precipitation were commonly superposed by temperature, and since the experiment site is well-drained, they were probably not very long-lasting. This is reflected by a low correlation of daily precipitation amount with CO_2 efflux, also when introducing time lags. Analogously, no significant correlation to wind speed was found.

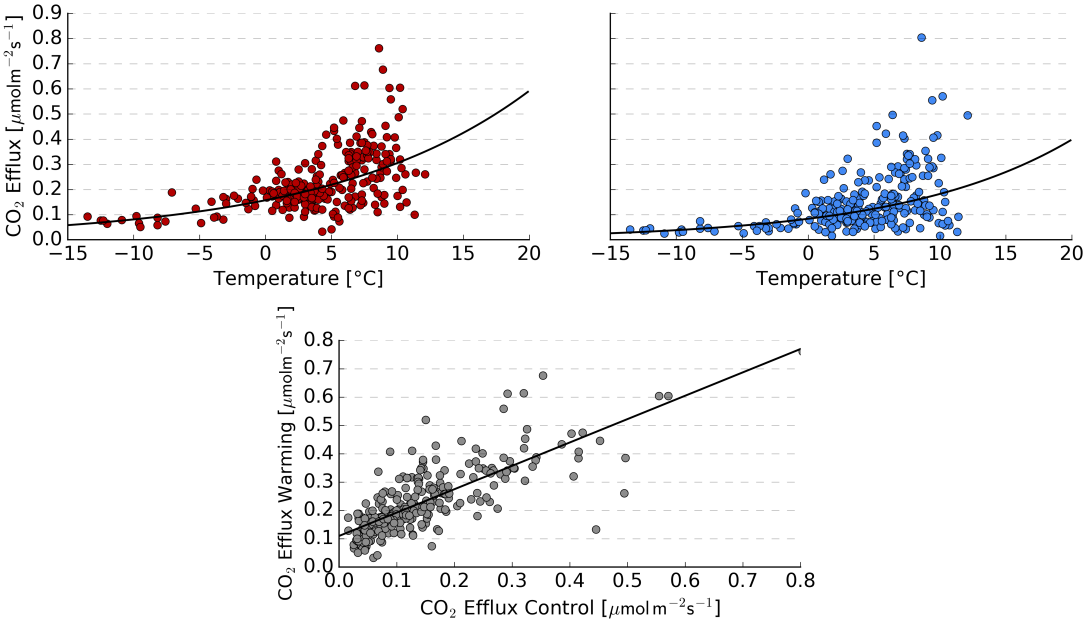

Figure 3.9: Upper plots: Dots indicate daily averaged soil CO_2 efflux in experimentally warmed (left side) and control (right side) sites, plotted against daily mean values of air temperatures measured at Longyearbyen airport. The result of a first-order exponential fit is depicted as solid black line. Lower plot: Daily averaged soil CO_2 efflux of control sites plotted against efflux of warmed sites.

3.5 Discussion

Considering weather patterns during the measurement campaign, particularly the winter 2015/16 and October 2016 were remarkable, as new pan-Arctic temperature records were set. The unprecedented temperature anomalies observed in the winter 2015/16 were related to the occurrence of a particularly strong low pressure system in the North Atlantic at the end of December 2015. The minimum core pressure was 928 hPa, the fourth-lowest value in the North Atlantic documented since 1958. It caused massive poleward transport of heat and moisture, which initiated a series of feedbacks that contributed to conserve warm anomalies in the Arctic, including the increase of downward longwave radiation by higher water vapour content and increased cloud cover, the erosion of surface inversions, and substantial sea ice loss (Overland et al., 2016; Kim et al., 2017). Furthermore, a long-lasting blocking regime directly following the low pressure system contributed to sustain high temperatures. The next autumn, again a persistent blocking system occurred over the north-east Atlantic and the Norwegian Sea, and several low pressure systems at the rear flank of the blocking system provided an influx of mild, moist air masses, leading to high temperatures and to the record

rainfall in the second half of 2016.

Seasonal trends of soil respiration were mostly controlled by temperature, which had the highest correlation with efflux of all tested environmental parameters. Even though air temperature data from a weather station located almost 10 km away from Endalen was used, the temperature response of soil respiration (Fig. 3.9) was explained relatively well. However, the reduced effect of temperature on respiration and the little day-to-day variation of effluxes in April and throughout autumn compared to the growing season are conspicuous (Fig. 3.8). While it is clear that the snow cover was the main reason for this phenomenon in April, the relatively constant effluxes in autumn could be related to the diminished solar input: Particularly on short time scales, photosynthetic activity and root exudations vary with irradiance, which is strongly affected by cloud coverage in the polar summer. A sequence of alternating cloudy and sunny days will therefore lead to considerable variation of soil CO_2 efflux, as observed during the growing season. In autumn, winter and early spring, solar input in Svalbard is generally negligibly small, hence the influence of a changing cloud cover is small, and effluxes can be relatively stable. Similarly, soil temperatures may also show greater day-to-day variation when the solar elevation angle is higher, since they respond stronger to irradiance changes than air temperature.

Apart from temperature, precipitation and soil water content also contributed to trigger increased respiration. The largest pulse of soil respiration was measured shortly after the biggest rainfall event during the measurement campaign; an observation that is consistent with other studies, which found sensitivity of respiration to wetting in high Arctic sites (Lupascu et al., 2014). In contrast, no major impacts of wind were found. However, as wind speed is spatially highly variable, it is likely that it differs significantly between the measurement location at Longyearbyen airport and the rather wind-protected Endalen valley, and wind speed observations in Endalen would be necessary to determine the influence of wind speed.

Concerning differences in respiration between warming and control sites, the data provides strong evidence that long-term experimental summertime warming caused an increase of soil respiration throughout spring, summer and parts of autumn. The sparse data of snow cover days also indicates a similar pattern in winter. It is difficult to relate the observed respiration increase to specific causes, due to the variety of effects and interactions which are triggered by warming. It is further complicated by the lack of soil temperature data for individual plots in Endalen, as air temperature measurements from Longyearbyen airport obviously do not account for the raised temperature in OTCs, so temperature effects on

respiration are difficult to resolve. However, adding 2 K, which is the upper limit of temperature increase possibly induced by OTCs, solely to temperature observations corresponding to efflux rates of warmed plots yields a result of enhanced soil respiration at a given temperature, so temperature stimulation of microbial activity alone is unlikely to have raised respiration. As long-term warming altered species composition, increased biomass and presumably favoured nitrogen mineralization inside the OTCs, changes in substrate quality, litter mass and root exudations could be the main drivers of increased effluxes. Furthermore, the slightly lower Q_{10} values of warmed plots (regardless of adding 2 K to temperature observations to account for OTC warming), could be a sign of microbial adaptation to a higher soil temperature level, or the microbial community has shifted.

The strongest relative increase of soil respiration in warmed plots occurred outside of the growing season, when air temperatures were comparably low. While it is likely that enhanced substrate quality and litter mass have contributed to this effect, it could also be partly caused by the reduction of extreme low temperature events by increased snow insulation, which is a side effect of OTC use. OTCs also reduce the frequency of freeze-thaw cycles, providing a possible explanation why efflux from control plots strongly exceeded efflux from OTC plots during snow melt on one day in early May 2016. Interestingly, efflux from control plots was also greater during some high-efflux events in late spring and summer 2016. Even the maximum daily mean efflux during the campaign was measured in control sites. This is probably linked to the microbial depletion of labile soil substrates on days with favourable environmental conditions, which could occur faster in warmed plots due to the enhanced microbial activity. In fact, detailed flux data of this particular day supports this hypothesis as it reveals that efflux in warmed plots was higher in the beginning of the day, but decreased faster than in control plots during the second half of the day, ultimately making the daily average slightly smaller.

Assessing the magnitude of high Arctic terrestrial feedbacks on climate change based on measurements of soil respiration and temperature alone is, of course, hardly feasible. Although the observations described herein indicate the potential of soil respiration stimulation by warming, the increase of carbon uptake by plant growth, which was not determined in the course of this experiment, could offset the carbon release from soils. Apart from that, it is worth noting that the comparatively rapid warming observed in Svalbard and other Arctic regions in recent decades already altered biogeochemical processes, and the experimental temperature increase induced by OTCs is merely an additional warming stimulation. Furthermore, OTCs cannot accurately simulate the seasonal patterns of warming observed in the course of climate change, as climate warming in the high Arctic is most pronounced in

winter.

In any case, the experiment has shown the potential of the passive FD chamber design for long-time, high-frequency measurements of soil CO_2 efflux rates in the high Arctic, given sufficient power supply to endure the polar night. Despite the relatively low ratio between efflux value and measurement error in this environment, daily averaged effluxes seem plausible and are correlated well with air temperature. Nevertheless, more than 10 % of the raw data had to be eliminated because efflux rates were negative, which is only possible when C_{atm} exceeds C_{chamb}. Over the course of the measurement campaign, negative effluxes were reported by all chambers, and frequently by more than one chamber at once, so if an error of an individual CO_2 concentration sensor was the reason, the device measuring C_{atm} must have been the source. However, since observations during the rest of the campaign were plausible and the devices were carefully calibrated, this is rather implausible. Pressure gradients between chamber and atmosphere, established during high wind speed events, are also an unlikely cause; although it could lead to an underestimation of efflux rate, the flux would still be directed from the soil into the chamber and thereby remain greater than zero. Perhaps, vegetation enclosed in the FD chamber was photosynthetically active, although this is improbable as well, as the inside should be completely dark. Alternatively, negative values in winter could occur when the soil membrane and the atmospheric membrane of the chamber are in different snow conditions, but due to the lack of power supply during winter, there were only a few snow cover days with available flux data in this measurement campaign, and many negative efflux values were recorded in other times of the year. Therefore, it remains largely unclear which effects led to the measured negative effluxes.

4 Land model simulations of a polar semi-desert

To quantify the effects of climate change on carbon fluxes between land and atmosphere in a polar semi-desert ecosystem in Svalbard, model simulations were conducted. After giving background information about the model, the results will be presented and discussed.

4.1 Introduction

Models simulating soil and land surface processes are an important component of today's Earth System Models, and are used to assess the impact of climate change on our environment and to predict terrestrial feedbacks to climate change. Furthermore, they can also be applied for site-level simulations, which aim to forecast biogeochemical processes of specific ecosystems in great detail. In order to answer open questions of the previous chapter and specify all major components of the carbon cycle, several simulations of the study site in Endalen, Svalbard were run. Specifically, the following points were addressed: How do land carbon uptake and release in a polar semi-desert respond to rapid Arctic warming? Will rising precipitation sums lead to increased carbon sequestration, or will other effects such as enhanced respiration offset plant growth?

4.2 Materials and methods

Version 4.5 of the Community Land Model was used for the site-level simulations. The model was developed in the late 1990s in an effort to establish a new, dynamic land component for the Community Climate System Model (CCSM), the climate model of the National Center for Atmospheric Research (NCAR) (Lawrence and Fisher, 2013). In 2010, the successor of

CCSM, the Community Earth System Model (CESM), was released, which incorporates CLM as its land surface model.

While the original intention was merely to provide a lower boundary condition for atmospheric simulations, CLM has grown to a sophisticated terrestrial system model, including several submodels for biogeochemistry, biogeophysics and many other processes. As component of an Earth System Model, the main purpose of a land model is firstly to simulate exchanges of energy, momentum, water, CO_2 and other trace gases between terrestrial ecosystems and the atmosphere; secondly to represent the state of the land surface, for example soil moisture or the distribution of carbon pools; and lastly, the land model should provide characteristics of the land surface, like surface roughness, leaf area index or emissivity (Lawrence, 2016). Most of the processes currently represented in CLM are depicted in Fig. 4.1. Owing to the detailed soil thermodynamics, hydrology and biogeochemistry schemes, CLM also resolves the effects of climate change on permafrost dynamics (Koven et al., 2015; Lawrence et al., 2015).

There are continuous efforts to improve model physics and parametrisations, although validation is difficult as long-term observations of biogeochemical quantities are sparse. Since land processes are tightly interwoven, it is also necessary to maintain a balanced scientific complexity across resolved processes (Lawrence and Fisher, 2013).

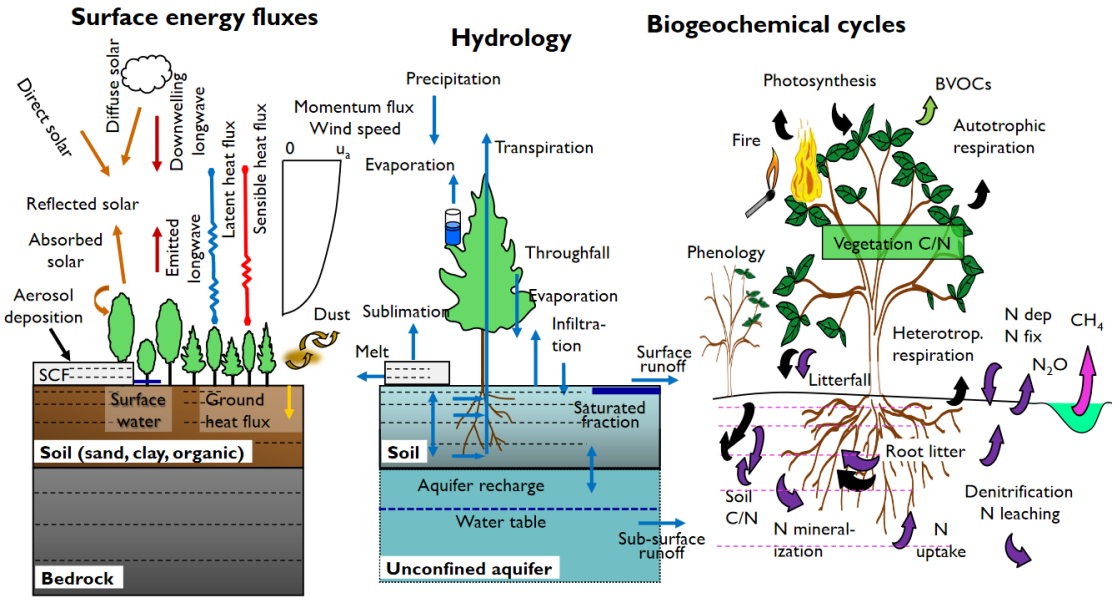

Figure 4.1: Schematic diagram of key processes simulated by CLM 4.5. On the right-hand side, black and pink arrows indicate carbon- and nitrogen-related processes, respectively. From Lawrence (2016).

The main field of application is still to be the terrestrial component of Earth System Models in coupled long-term simulations, as part of CESM and the Norwegian Earth System Model, NorESM. In this use case, the atmospheric forcing is obtained from the coupled atmospheric model, to which fluxes of energy, momentum, water and other quantities are passed back. However, CLM is being increasingly applied to assess climate change impacts on ecosystems at various spatio-temporal scales in independent, so-called offline simulations, for example to quantify future water resources or special land feedback processes like permafrost thawing. Here, CLM is not necessarily coupled with other model components, and the atmospheric forcing is often a prescribed dataset.

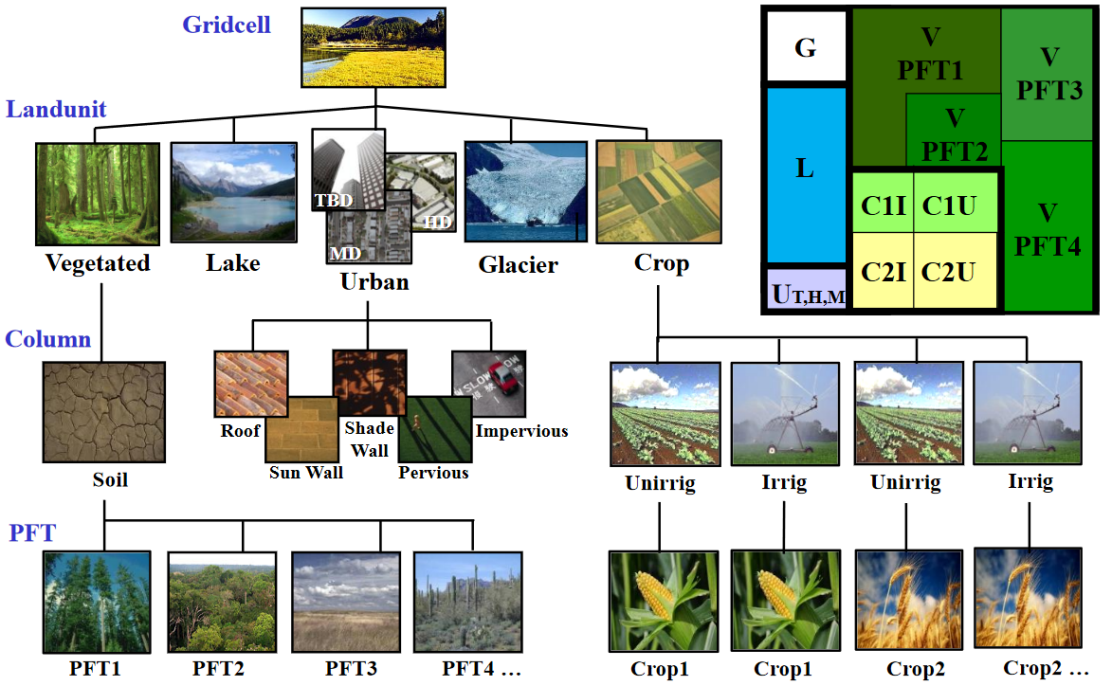

Figure 4.2: Schematic of land cover types and their sub-grid distribution in CLM 4.5. From Wieder et al. (2016).

For this study, CLM 4.5 was run in single-point resolution on a Cray XE6m-200 supercomputer operated by the University of Bergen, Norway. Again, Endalen (78.2°N, 15.7°E) was chosen as location. After creating the surface data map, which specifies land coverage based on CLM land-unit types (see Fig. 4.2), two spin-up simulations were made to create initial conditions for the actual model experiments. The CRU-NCEP.v4 reanalysis, which combines CRU TS and NCEP reanalysis data sets and is often used for the purpose of land model simulations, served as atmospheric forcing for both spin-ups (Viovy, 2011).

The first spin-up with a simulation length of 1000 years was run in accelerated mode, fol-

Notation	Scenario
CTR	Actual atmospheric forcing
T1	+1 K temperature
T2	+2 K temperature
T4	+4 K temperature
P25	+25 % precipitation
T1P25	+1 K temperature and +25 % precipitation
T2P25	+2 K temperature and +25 % precipitation
T4P25	+4 K temperature and +25 % precipitation

Table 4.1: Nomenclature used herein for different atmospheric forcing scenarios.

lowed by the second spin-up in normal mode simulating 200 more years. For these two spin-ups, data from 1901 to 1920 in 6-hourly resolution was cycled over the entire simulation period. The results of the second spin-up served as initial condition for another run, which simulated the ecosystem from 1901 until 1991, forced by corresponding CRU-NCEP reanalysis data. In contrast to the spin-up, variable atmospheric CO_2 concentrations were allowed in this simulation. Starting from 1991 and ending with 2010, different scenarios regarding atmospheric temperature and precipitation were tested: (1) A control experiment with actual atmospheric forcing, (2) an increase of air temperature of 1 K, (3) an increase of 2 K, (4) an increase of 4 K, (5) a precipitation increase of 25 %, (6) a precipitation increase of 25 % and a temperature increase of 1 K, (7) a precipitation increase of 25 % and a temperature increase of 2 K, (8) a precipitation increase of 25 % and a temperature increase of 4 K (see Tab. 4.1). The manipulations were implemented by adding a constant temperature factor to CRU-NCEP 2m temperature and/or by multiplying CRU-NCEP precipitation data by 25 %. All changes were applied to full extent from the first day of the simulation onward, because the temperature manipulations should be comparable to temperature increases by OTCs, which are also immediately effective.

4.3 Results

4.3.1 Carbon uptake

All warming scenarios resulted in an increase of photosynthesis and primary production, with largest enhancement under the warmest, 4 K scenarios. GPP in warming simulations already rose in the first year of the model simulation and remained higher than the control

until the end of the simulation (see Fig. 4.6). Clearly, the temperature increase lengthened the growing season and particularly enhanced GPP during late spring and early summer (see Fig. 4.3), as the snow melt occurred earlier in the year (see Fig. 4.4). In May, the average GPP of the T4 scenario was 102 $g C m^{-2}$, whereas it was just 2.5 $g C m^{-2}$ in the control experiment. The relative increase was smaller during the rest of the growing season: While the average July GPP in the T4 experiment was still 80 % higher compared to the control simulation, the GPP in August increased by only 16 %. The growing season is also extended into autumn, but the GPP increase is less distinct than in spring. A similar annual pattern as in the 4 K scenarios is detectable in the other warming scenarios as well, although less pronounced.

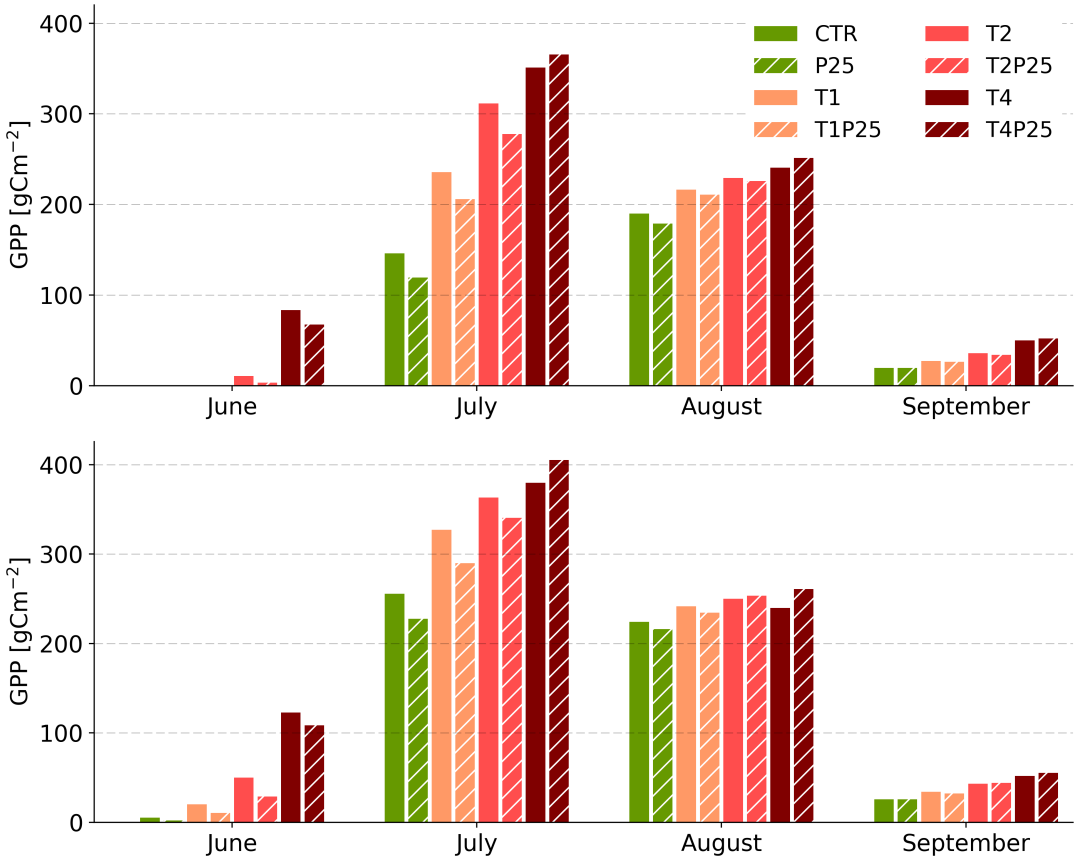

Figure 4.3: Average monthly GPP during growing season in each scenario between 1991-2000 (upper plot) and 2001-2010 (lower plot). Hatched bars indicate simulations with 25 % precipitation increase.

The 25 % increase of precipitation slightly reduced simulated annual primary production in most cases, particularly in scenarios with little or no temperature change. Solely in the T4P25 scenario, it resulted in a 3 % GPP increase compared to its counterpart without precipitation

addition, averaged over the entire simulation period. In contrast, GPP decreased by 9 % in the P25 scenario relative to the control simulation. The decrease was strongest in spring, suggesting that the increase of snowfall, which comes along with the precipitation increase, shortens the growing season by prolonging the snow cover duration and inhibits primary production in late spring. The mean snow depth in June, for example, increased between 33 % to 69 % after precipitation addition (see Fig. 4.4). However, rising temperatures make the ecosystem more prone to water limitation by promoting evapotranspiration, and above a certain temperature threshold, the effect of prolonged snow cover duration on plant growth is eventually outweighed by the enhanced soil moisture. This inference is supported by the simulated volumetric soil water content, which was by far lowest in the T4 scenario.

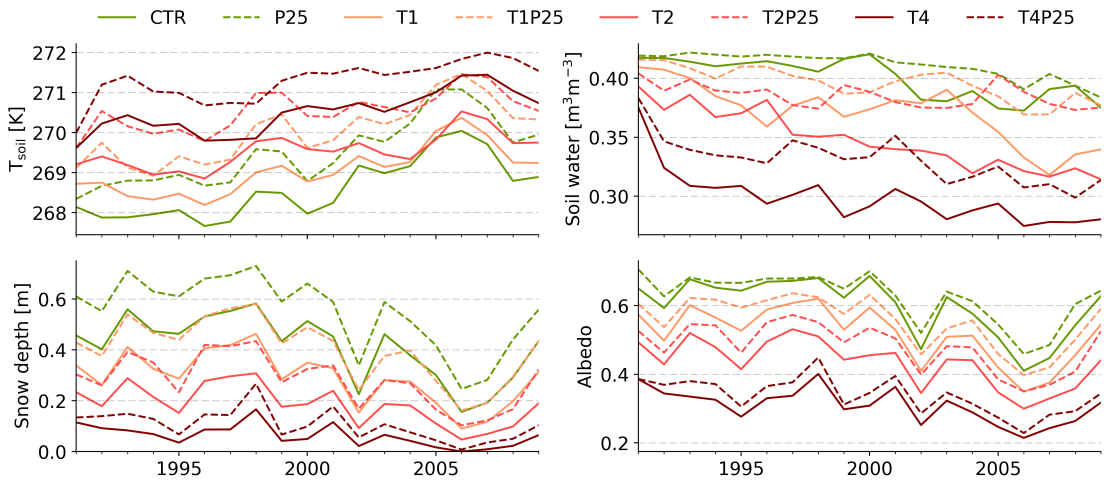

Figure 4.4: Time series of environmental parameters between 1991 and 2010, as modelled by CLM. The upper plots depict annual averages of soil temperature and volumetric soil water content at a depth of 10 cm. The lower left plot depicts mean snow depth in June and the lower right plot albedo in June. Dashed lines indicate simulations with precipitation increase, while solid lines denote the control and warming-only simulations.

Most of the interannual variation of primary production was attributable to air temperature fluctuations (R^2 between 0.65 and 0.75, depending on scenario), while little impact of precipitation was found. A significant trend of GPP between 1991 and 2010 was simulated in all model experiments, concurring with pronounced Arctic warming of approximately 2.5 K within two decades. Across all experiments, average GPP of the period 2007-2009 was 100 g C m^{-2} yr^{-1} to 150 g C m^{-2} yr^{-1} higher than between 1991 and 1993. The increase (both relative and by absolute numbers) was smallest under the T4 and T4P25 scenarios, and relatively largest in the control and P25 simulations. In the warming experiments, the adaptation of primary production to the abruptly enhanced temperature levels after simulation start

was fast and mostly occurred within the first three years of the simulation, followed by a period of stagnating GPP until the late 1990s. Subsequently, GPP rose again, particularly in the experiments with modest or no artificial temperature addition. In the control experiment with ambient atmospheric forcing, a remarkable increase of annual GPP of 46 % – again comparing 1991-1993 and 2007-2009 – was simulated. The largest part of the increase took place in the 2000s, coinciding with the markedly Arctic warming in this decade (see Fig. 4.6).

4.3.2 Carbon loss

As primary production, carbon loss by respiration is promoted by higher temperatures. Consequently, highest autotrophic and heterotrophic respiration were simulated in the T4 and T4P25 model experiments, and lowest under the scenarios without temperature manipulation (see Fig. 4.6). Increased decomposition in the warming simulations also caused higher nitrogen mineralization rates, providing nutrients to support plant growth. Nitrogen mineralization was particularly enhanced in the beginning and at the end of the growing season (see Fig. 4.5).

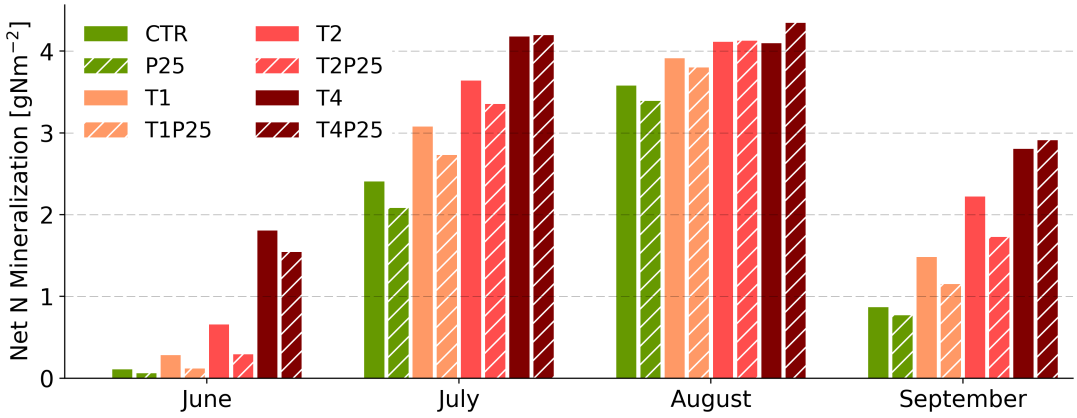

Figure 4.5: Average monthly net nitrogen mineralization during growing season between 1991-2010. Hatched bars indicate simulations with 25 % precipitation increase.

Expectedly, autotrophic respiration correlated well with primary production, whereas the effects of increased biomass on heterotrophic respiration are mediated by litter mass and quality, causing a different temporal pattern in response to warming. While autotrophic respiration increased strongly between the first and the third year of the simulation in all warming scenarios – due to enhanced plant growth and biomass increase – heterotrophic

respiration stagnated until 1994, after it had already been stimulated in the first year of simulation by elevated soil temperatures. After 1994, the rising litter mass and substrate quality came into effect and caused increasing heterotrophic respiration in the mid-1990s. Average heterotrophic respiration during the last four years of the model simulation was higher in the T2 scenario than in the T4 scenario, probably the result of moisture limitation in the T4 scenario. Considering the annual cycle, ecosystem respiration (i.e., the sum of autotrophic and heterotrophic respiration) in the warming experiments was particularly enhanced in spring and autumn, as the growing season was prolonged by atmospheric warming. Conforming with the fact that microbial activity is supported over a broader temperature range than plant growth, heterotrophic respiration strongly exceeded autotrophic respiration in spring and autumn, while their magnitude was similar during midsummer. In winter, neither autotrophic nor substantial heterotrophic respiration were simulated, regardless of the soil temperature.

Analogously to the effects on GPP, increasing precipitation by 25 % reduced autotrophic and heterotrophic respiration in most of the scenarios; only in the T4P25 simulation, wetting enhanced carbon loss. Reduced ecosystem respiration after adding precipitation seems implausible, considering that wetting enhanced soil temperatures (see Fig. 4.4), which would suggest increased microbial activity and more favourable environmental conditions for plant growth. However, the soil temperature increase was by far largest during winter, as the thicker snow cover insulated the soil more effectively, whereas the soil temperature even was slightly reduced at the beginning of the growing season due to the extended snow cover duration. Since simulated heterotrophic respiration during winter was generally very low, the temperature increase had only little consequences for the annual carbon release by respiration. However, plant growth was constrained by the delayed snow melt, and subsequently, litter mass and quality were presumably lower in the experiments with increased precipitation, reducing both autotrophic and heterotrophic respiration. This conclusion is supported by the seasonal pattern of respiration: The reduction of ecosystem respiration after adding precipitation was most pronounced in spring, while respiration in autumn even was somewhat higher under increased precipitation conditions in all experiments.

As the combined result of belowground autotrophic and heterotrophic respiration, the response of soil respiration is mainly a superposition of the results described above. Atmospheric warming drastically increased the amount of carbon released from the soil: Summed up over the entire simulation period, warming by 1 K (without adding precipitation) enhanced soil respiration by 23 %, 2 K by 42 % and 4 K by 57 %. Increasing precipitation generally lowered soil respiration, except for the T4P25 scenario. The amount of methane

released from soil was negligible, and did not differ significantly between the experiments.

Under the T4 and T4P25 scenarios, considerable wildfire emissions up to 400 $gC\,m^{-2}\,yr^{-1}$ – approximately 50 % of GPP – were simulated towards the end of the simulation period, while wildfires were of minor importance in all other simulations.

4.3.3 Carbon balance

NEP was clearly positive throughout the simulation in all warming experiments, and in 17 out of 19 years also in the two simulations without temperature change (see Fig. 4.6). Since other non-gaseous carbon fluxes are comparably low (leaving aside simulated wildfire emissions), this is an indication that the ecosystem already accumulated carbon under ambient atmospheric conditions, but particularly under strong warming. The highest total ecosystem production was simulated in the T4 experiment with an average NEP of 122 $gC\,m^{-2}\,yr^{-1}$, while only 33 $gC\,m^{-2}\,yr^{-1}$ and 28 $gC\,m^{-2}\,yr^{-1}$ accumulated in the control and P25 experiment, respectively.

On average, NEP was highest in July and August, increasing with artificial temperature enhancement, and decreasing with additional precipitation. Moderately negative NEP was simulated both after snow melt and in early autumn, at the end of the growing season. These short periods of negative NEP may have been caused by the efflux of soil CO_2 that had accumulated under the snow cover in spring and decomposition of litter in autumn. The negative phases were more pronounced in warmed conditions, while the increase of precipitation did not play a significant role. In winter, neither primary production nor substantial ecosystem respiration occurred, and NEP was therefore almost zero.

During the first years after simulation start, annual NEP was highly positive in all simulations in which temperature was increased. The abrupt change of atmospheric forcing clearly favoured plant growth and carbon sequestration in plants, while carbon loss by heterotrophic respiration initially did not increase at the same rate. However, after approximately five years the ecosystem reached a slightly more balanced state under the warming scenarios, as heterotrophic respiration increased, while primary production stagnated. Subsequently, annual NEP remained low – in the control and P25 experiment partly negative – until the early 2000s, when GPP began to increase again, as described above. In contrast to the 1990s, when differences between the scenarios were pronounced, NEP varied relatively little among model experiments during the last eight years of the simulation; the T4 and T4P25 scenarios were a notable exception, as their total NEP during this time was twice as high as in every

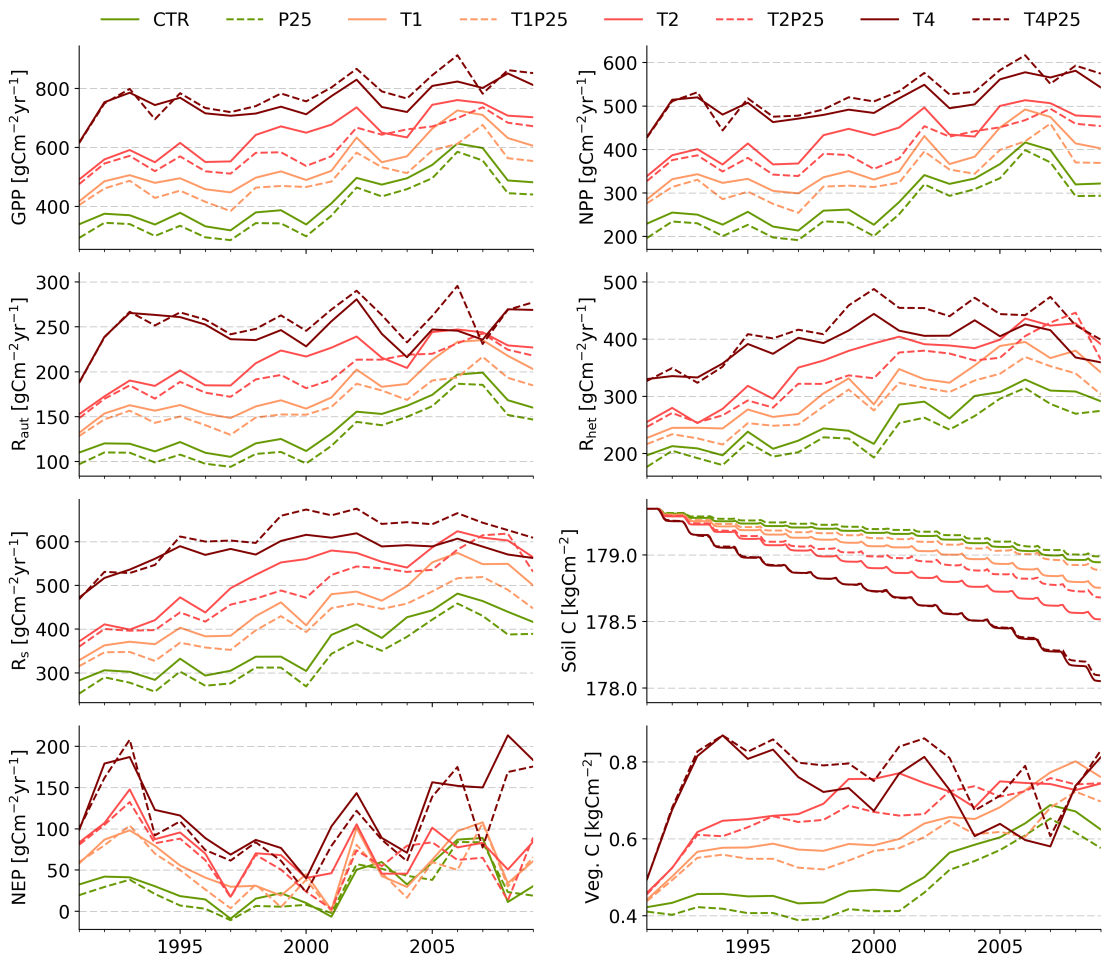

Figure 4.6: Time series of key quantities of the terrestrial carbon cycle between 1991 and 2010, as modelled by CLM. Dashed lines indicate simulations with precipitation increase, while solid lines denote the control and warming-only simulations.

other scenario. Since significant carbon losses by wildfire were simulated in these scenarios, the high NEP could reflect post-disturbance carbon accumulation.

In all experiments, additional carbon was stored in new plant biomass, coinciding with an increase of leaf area index and canopy height. The simulated effects of greening on the summer albedo were negligible; however, the shortening of the snow cover duration drastically reduced the albedo in spring, particularly in the T2 and T4 experiments (see Fig. 4.4).

In contrast to vegetation biomass, soil carbon content decreased in every model simulation, indicating loss of older soil organic matter. The loss increased with temperature addition and

was reduced by precipitation increase; vice versa, carbon storage in plants was enhanced by temperature increase, but decreased by adding precipitation. Wildfire constituted a significant part of the carbon balance in the 4 K warming simulations, and turned the ecosystem from a net carbon sink to a source for the atmosphere in the 2000s. Moreover, it substantially decreased plant biomass during that period.

4.4 Discussion

The model simulations clearly illustrated potential consequences of atmospheric warming on the carbon cycle in polar semi-deserts. Artificial warming as well as actual warming of the lower troposphere, which was particularly strong in the 2000s, caused a massive increase of primary production and enhanced rates of biogeochemical processes. The simulated ecosystem response to experimental warming was remarkably strong and fast, highlighting the sensitivity of polar semi-deserts to climate change. Already in the first year of simulation, annual GPP differences between the scenarios up to 300 $\mathrm{g\,C\,m^{-2}\,yr^{-1}}$ were modelled. However, it is unclear if real-world ecosystems would respond at this rate, or if the adaptation to a warmer climate would require more time.

Simulated GPP and NPP were relatively high compared to typical values observed in the high Arctic (Stiling, 1996; Chapin et al., 2011), and cannot be verified for the study site due to lack of observational data. Another rather unexpected feature of the model experiments was the reduction of NPP after adding precipitation, conflicting with the results of long-term measurements at a similar latitude (Lupascu et al., 2014). Nonetheless, the model simulations are not entirely implausible: The prolonged snow cover period in spring could affect plant growth more strongly than the slightly increased soil moisture in summer does, as soil water content in Endalen is relatively high anyway. Undoubtedly, the validity of this finding depends on the accuracy of snow cover dynamics in CLM. In this regard, a comparison with observations shows that simulated snow depths could be overestimated. In the control simulation, average snow depth in April – typically one of the months with highest snow depth – between 1991 and 2010 was 80 cm, although the snow depth in the area of Longyearbyen is rarely higher than 50 cm due to strong winds. Moreover, June is usually largely snow-free, but average snow depths above 30 cm were simulated in the control experiment. Therefore, it is likely that the timing of snow melt was modelled wrongly, although it is crucial for all ecosystem processes.

Comparison of model output to the soil CO_2 efflux observations described in section 3.4 reveals substantial differences of soil respiration of one order of magnitude during midsummer. While cumulated soil CO_2 efflux in control and warming sites in July 2016 was 27 $gC\,m^{-2}$ and 37 $gC\,m^{-2}$, respectively, average model soil respiration in July was as high as 150 $gC\,m^{-2}$ in the control simulation and 185 $gC\,m^{-2}$ under the T1 scenario, which should correspond well to the temperature change induced by OTCs. Similar to primary production, autotrophic respiration in the soil and microbial decomposition may be overestimated. On the contrary, soil respiration in winter could be underestimated in the model, as total monthly efflux in winter was smaller than 1 $gC\,m^{-2}$, whereas observations in Endalen suggest wintertime soil CO_2 effluxes in the order of 3 $gC\,m^{-2}$ to 5 $gC\,m^{-2}$ per month, although only April data was used for this assessment, as soil CO_2 efflux measurements could not be conducted between mid-October and April. Comparing the relative change induced by warming, agreement between observations and model results is slightly higher. Average soil CO_2 efflux rates increased by 23 % between the control and T1 scenario, while they increased by 60 % between warming and control plots in the measurement campaign. The seasonal pattern of soil respiration enhancement was partly replicated by the land model, with maximum change in winter and early spring and smaller increase in the summertime – however, the magnitude of increase in May and June was substantially overestimated by the model, which simulated 3.3 times higher soil CO_2 efflux rates in May under the T1 scenario (averaged over the full simulation length), while only 1.2 times more CO_2 was released from warming plots in Endalen in May 2016. However, deviations between model output and observations are often associated with the error of representativeness, which could be particularly large in this case, considering that spatio-temporal variation of soil CO_2 efflux is high and the slope of Endalen valley may not be representative for the surroundings. Apart from that, a longer observational time series would be necessary for a more profound assessment of model-observation differences.

Significant carbon losses by wildfire, linked to low fuel moisture, were simulated in the 4 K warming experiments. The wildfire model has been revised in CLM4.5 and provides reasonable estimates of global wildfire carbon loss (Li et al., 2014), but to the author's knowledge, no studies about possible biases in the high Arctic exist at the moment. Tundra wildfires frequently occur in continental, shrub-dominated areas of northern Canada and in Alaska, but have not been reported in Svalbard so far. It seems unlikely that fuel load would suffice to support larger wildfires, even if plant biomass increases. As a consequence, T4 and T4P25 model outputs of carbon fluxes should be considered as highly uncertain, particularly in the 2000s, when huge carbon losses by wildfires were simulated.

The results of the simulations cannot be applied directly to assess the future pathway of carbon fluxes in polar semi-deserts. Firstly, the temperature increase in the warming experiments was introduced abruptly, from one year to the next. Real-world climate change, of course, is slower and more gradual, causing different patterns of plant responses and ecosystem consequences, as observable in the control simulation, which was subject to ambient warming only. Secondly, warming by climate change varies from season to season and is – in Arctic regions – generally more pronounced in winter and less extreme in spring, when largest GPP increases were modelled in this experiment. Precipitation trends are highly uncertain as well, and seasonal variation could be crucial considering the control exerted by the snow cover or possible moisture limitations during the growing season. Lastly, CLM was not coupled with an atmospheric model; therefore, feedback processes between land and atmosphere were not represented in the model simulation. For instance, prolonging the snow cover duration should have reduced the temperature in the lower troposphere, as more solar radiation is reflected. Since atmospheric forcing was prescribed, this could not be taken into account – soil temperature, however, was affected, as it is internally modelled by CLM.

Considering these restrictions, only cautious statements about the future carbon balance in the polar semi-desert environment of Endalen can be made. It is likely that the rates of the two major processes controlling the carbon exchange between land and atmosphere – photosynthesis and respiration – will continue to increase in the next decades, thus accelerating land carbon cycling and other biogeochemical processes. Although a considerable amount of soil carbon was lost through the stimulation of microbial activity, carbon sequestration in plants increased more strongly in every simulation, suggesting that polar semi-deserts will act as carbon sinks in the near future, and remove CO_2 from the atmosphere; a conclusion that is similar to the findings of CMIP5. An increase of precipitation, which is projected for Arctic regions until the end of this century, could counteract the effects of warming by slightly prolonging the duration of snow cover and shortening the growing season. However, there is an opposing process, as warming makes the ecosystem susceptible to moisture limitation. Therefore, more precipitation could stimulate plant growth over the long term, particularly when the temperature increase is pronounced.

5 Summary

Both experiments that were described in this thesis – an observation-based and a model-based one – have indicated potential consequences of climate change on the carbon cycle in Arctic terrestrial ecosystems. These ecosystems will undergo massive changes in the course of climate change; on the one hand, as global warming in the Arctic is amplified by several feedback processes, on the other hand, as they are sensitive to environmental changes, since plant growth is currently strongly limited by temperature, and concurring processes on the land surface and in the soil will probably increase the absorption of solar radiation and the availability of nutrients.

Measurements of soil CO_2 efflux with a recently developed, automated forced-diffusion dynamic chamber in a valley near Longyearbyen have shown that soil respiration increased in a controlled warming environment, likely due to enhanced microbial respiration and increased autotrophic respiration, the latter being caused by the stimulation of plant growth. The difference between warmed and control plots was most pronounced outside of the growing season. The increased soil carbon loss in the warmed plots may have been offset by higher carbon input through primary production, which has not been measured in the course of the experiment.

Site-level simulations run with the current version of the NCAR-developed Community Land Model (CLM4.5) in the period between 1991 and 2010 were used to assess the effects of climate change on other components of the carbon cycle as well. Experimental warming amplified the rates of biogeochemical processes and enhanced both carbon uptake and carbon loss from the ecosystem, but in general, more carbon was sequestered. Artificial warming was partly overlain by the drastic temperature increase that took place in the Arctic during the time of the simulation, which led to carbon sequestration in the control run as well. Increasing precipitation sums in the Arctic, which are expected in the future, but – in contrast to warming – have not been observed yet, could diminish plant growth and ecosystem respiration through effects on snow cover duration. Overall, the simulations suggest that polar semi-deserts comparable to the study site on Spitsbergen will act as carbon sinks under ongoing climate change, at least in the near future.

Bibliography

Allison, S. D. (2006). 'Brown Ground: A Soil Carbon Analogue for the Green World Hypothesis?' In: *The American Naturalist* 167.5, pp. 619–627.

Anthony, K. M. W. et al. (2014). 'A shift of thermokarst lakes from carbon sources to sinks during the Holocene epoch'. In: *Nature* 511.7510, pp. 452–456.

Baltzer, J. L. et al. (2014). 'Forests on thawing permafrost: fragmentation, edge effects, and net forest loss'. In: *Global change biology* 20.3, pp. 824–834.

Belshe, E. F. et al. (2013). 'Tundra ecosystems observed to be CO2 sources due to differential amplification of the carbon cycle'. In: *Ecology Letters* 16.10, pp. 1307–1315.

Beringer, J. et al. (2005). 'Surface energy exchanges along a tundra-forest transition and feedbacks to climate'. In: *Agricultural and Forest Meteorology* 131.3, pp. 143–161.

Billings, W. D. et al. (1977). 'Root Growth, Respiration, and Carbon Dioxide Evolution in an Arctic Tundra Soil'. In: *Arctic and Alpine Research* 9.2, pp. 129–137.

Bintanja, R. and F. M. Selten (2014). 'Future increases in Arctic precipitation linked to local evaporation and sea-ice retreat'. In: *Nature* 509.7501, pp. 479–482.

Bintanja, R. et al. (2012). 'Boundary layer stability and Arctic climate change: a feedback study using EC-Earth'. In: *Climate Dynamics* 39.11, pp. 2659–2673.

Bokhorst, S. et al. (2013). 'Variable temperature effects of Open Top Chambers at polar and alpine sites explained by irradiance and snow depth'. In: *Global Change Biology* 19.1, pp. 64–74.

Bond-Lamberty, B. and A. Thomson (2010). 'Temperature-associated increases in the global soil respiration record'. In: *Nature* 464.7288, pp. 579–582.

Bradford, M. A. et al. (2008). 'Thermal adaptation of soil microbial respiration to elevated temperature'. In: *Ecology Letters* 11.12, pp. 1316–1327.

Callaghan, T. et al. (2005). 'Arctic tundra and polar desert ecosystems'. In: *Arctic climate impact assessment*. Cambridge, New York: Cambridge University Press, pp. 243–352.

Chapin, F. S. et al. (2011). *Principles of terrestrial ecosystem ecology*. 2nd ed. New York: Springer. 529 pp.

Davidson, E. A. et al. (2002). 'Minimizing artifacts and biases in chamber-based measurements of soil respiration'. In: *Agricultural and Forest Meteorology*. FLUXNET 2000 Synthesis 113.1, pp. 21–37.

Elberling, B. (2007). 'Annual soil CO2 effluxes in the High Arctic: The role of snow thickness and vegetation type'. In: *Soil Biology and Biochemistry* 39.2, pp. 646–654.

Elberling, B. and K. K. Brandt (2003). 'Uncoupling of microbial CO2 production and release in frozen soil and its implications for field studies of arctic C cycling'. In: *Soil Biology and Biochemistry* 35.2, pp. 263–272.

Fang, C. and J. B. Moncrieff (2001). 'The dependence of soil CO2 efflux on temperature'. In: *Soil Biology and Biochemistry* 33.2, pp. 155–165.

Førland, E. J. et al. (2012). 'Temperature and precipitation development at Svalbard 1900–2100'. In: *Advances in Meteorology* 2011.

Goetz, S. J. et al. (2005). 'Satellite-observed photosynthetic trends across boreal North America associated with climate and fire disturbance'. In: *Proceedings of the National Academy of Sciences of the United States of America* 102.38, pp. 13521–13525.

Grant, R. F. and P. Rochette (1994). 'Soil Microbial Respiration at Different Water Potentials and Temperatures: Theory and Mathematical Modeling'. In: *Soil Science Society of America Journal* 58.6, p. 1681.

Grogan, P. and F. S. Chapin (1999). 'Arctic Soil Respiration: Effects of Climate and Vegetation Depend on Season'. In: *Ecosystems* 2.5, pp. 451–459.

Grogan, P. (2012). 'Cold Season Respiration Across a Low Arctic Landscape: the Influence of Vegetation Type, Snow Depth, and Interannual Climatic Variation'. In: *Arctic, Antarctic, and Alpine Research* 44.4, pp. 446–456.

Grogan, P. and S. Jonasson (2006). 'Ecosystem CO2 production during winter in a Swedish subarctic region: the relative importance of climate and vegetation type'. In: *Global Change Biology* 12.8, pp. 1479–1495.

Grosse, G. et al. (2013). 'Distribution of late Pleistocene ice-rich syngenetic permafrost of the Yedoma Suite in east and central Siberia, Russia'. In: *US Geological Survey Open File Report* 2013.1078, pp. 1–37.

Hartley, I. P. et al. (2007). 'Effects of three years of soil warming and shading on the rate of soil respiration: substrate availability and not thermal acclimation mediates observed response'. In: *Global Change Biology* 13.8, pp. 1761–1770.

Hashimoto, S. et al. (2015). 'Global spatiotemporal distribution of soil respiration modeled using a global database'. In: *Biogeosciences* 12.13, pp. 4121–4132.

Heimann, M. and M. Reichstein (2008). 'Terrestrial ecosystem carbon dynamics and climate feedbacks'. In: *Nature* 451.7176, pp. 289–292.

Henry, G. and U. Molau (1997). 'Tundra plants and climate change: the International Tundra Experiment (ITEX)'. In: *Global Change Biology* 3 (S1), pp. 1–9.

Hoerling, M. P. et al. (2001). 'Tropical Origins for Recent North Atlantic Climate Change'. In: *Science* 292.5514, pp. 90–92.

Horwath, J. and R. S. Sletten (2010). 'Spatial distribution of soil organic carbon in northwest Greenland and underestimates of high Arctic carbon stores'. In: *Global Biogeochemical Cycles* 24.3, GB3012.

Houlton, B. Z. et al. (2008). 'A unifying framework for dinitrogen fixation in the terrestrial biosphere'. In: *Nature* 454.7202, pp. 327–330.

Hugelius, G. et al. (2014). 'Estimated stocks of circumpolar permafrost carbon with quantified uncertainty ranges and identified data gaps'. In: *Biogeosciences* 11.23, pp. 6573–6593.

IPCC (2013). *Climate Change 2013: The Physical Science Basis. Working Group I Contribution to the Fifth Assessment Report of the Intergovernmental Panel on Climate Change*. Cambridge: Cambridge University Press.

Jonasson, S. and A. Michelsen (1996). 'Nutrient Cycling in Subarctic and Arctic Ecosystems, with Special Reference to the Abisko and Torneträsk Region'. In: *Ecological Bulletins* 45, pp. 45–52.

Jonasson, S. et al. (2001). 'Biogeochemistry in the Arctic: Patterns, Processes and Controls'. In: *Global Biogeochemical Cycles in the Climate System*. New York: Academic Press, pp. 139–150.

Kim, B.-M. et al. (2017). 'Major cause of unprecedented Arctic warming in January 2016: Critical role of an Atlantic windstorm'. In: *Scientific Reports* 7, p. 40051.

Klaus, K. (2016). 'A novel approach to measure microbial carbon use efficiency by estimating growth from 18O incorporation into DNA'. Master's Thesis. Vienna: University of Vienna. 66 pp.

Knoblauch, C. et al. (2013). 'Predicting long-term carbon mineralization and trace gas production from thawing permafrost of Northeast Siberia'. In: *Global Change Biology* 19.4, pp. 1160–1172.

Köppen, W. (1931). *Grundriss der Klimakunde*. W. de Gruyter.

Koven, C. D. et al. (2015). 'Permafrost carbon-climate feedback is sensitive to deep soil carbon decomposability but not deep soil nitrogen dynamics'. In: *Proceedings of the National Academy of Sciences* 112.12, pp. 3752–3757.

Landsberg, J. J. and S. T. Gower (1997). *Applications of physiological ecology to forest management*. Physiological ecology. San Diego: Academic Press. 354 pp.

Lawrence, D. M. (2016). 'Overview of the Community Land Model'.

Lawrence, D. M. and R. Fisher (2013). 'The Community Land Model Philosophy: model development and science applications'. In: *iLEAPS Newsletter* 13, pp. 16–19.

Lawrence, D. M. et al. (2015). 'Permafrost thaw and resulting soil moisture changes regulate projected high-latitude CO_2 and CH_4 emissions'. In: *Environmental Research Letters* 10.9, p. 094011.

Leirós, M. C. et al. (1999). 'Dependence of mineralization of soil organic matter on temperature and moisture'. In: *Soil Biology and Biochemistry* 31.3, pp. 327–335.

Li, F. et al. (2014). 'Quantifying the role of fire in the Earth system'. In: *Biogeosciences; Katlenburg-Lindau* 11.5.

Lloyd, J. and J. A. Taylor (1994). 'On the Temperature Dependence of Soil Respiration'. In: *Functional Ecology* 8.3, p. 315.

Lupascu, M. et al. (2014). 'High Arctic wetting reduces permafrost carbon feedbacks to climate warming'. In: *Nature Climate Change* 4.1, pp. 51–55.

Luyssaert, S. et al. (2007). 'CO2 balance of boreal, temperate, and tropical forests derived from a global database'. In: *Global Change Biology* 13.12, pp. 2509–2537.

Mack, M. C. et al. (2004). 'Ecosystem carbon storage in arctic tundra reduced by long-term nutrient fertilization'. In: *Nature* 431.7007, pp. 440–443.

Mack, M. C. et al. (2011). 'Carbon loss from an unprecedented Arctic tundra wildfire'. In: *Nature* 475.7357, pp. 489–492.

Marion, G. et al. (1997). 'Open-top designs for manipulating field temperature in high-latitude ecosystems'. In: *Global Change Biology* 3 (S1), pp. 20–32.

Mayer, M. et al. (2016). 'Facets of Arctic energy accumulation based on observations and reanalyses 2000–2015'. In: *Geophysical Research Letters* 43.19, 2016GL070557.

McBean, G. et al. (2005). 'Arctic Climate: Past and Present'. In: *Arctic climate impact assessment*. Cambridge, New York: Cambridge University Press, pp. 21–60.

McGuire, A. D. et al. (2009). 'Sensitivity of the carbon cycle in the Arctic to climate change'. In: *Ecological Monographs* 79.4, pp. 523–555.

McGuire, A. D. et al. (2010). 'An analysis of the carbon balance of the Arctic Basin from 1997 to 2006'. In: *Tellus B* 62.5, pp. 455–474.

McGuire, A. D. et al. (2012). 'An assessment of the carbon balance of Arctic tundra: comparisons among observations, process models, and atmospheric inversions'. In: *Biogeosciences* 9.8, pp. 3185–3204.

Mikan, C. J. et al. (2002). 'Temperature controls of microbial respiration in arctic tundra soils above and below freezing'. In: *Soil Biology and Biochemistry* 34.11, pp. 1785–1795.

NOAA (2017). *Arctic Oscillation*. URL: http://www.cpc.ncep.noaa.gov/products/precip/CWlink/daily_ao_index/ao.shtml (visited on 11/04/2017).

Nobrega, S. and P. Grogan (2007). 'Deeper Snow Enhances Winter Respiration from Both Plant-associated and Bulk Soil Carbon Pools in Birch Hummock Tundra'. In: *Ecosystems* 10.3, pp. 419–431.

Oechel, W. C. et al. (2000). 'Acclimation of ecosystem CO2 exchange in the Alaskan Arctic in response to decadal climate warming'. In: *Nature* 406.6799, pp. 978–981.

Olefeldt, D. et al. (2013). 'Environmental and physical controls on northern terrestrial methane emissions across permafrost zones'. In: *Global Change Biology* 19.2, pp. 589–603.

Overland, J. E. and M. Wang (2010). 'Large-scale atmospheric circulation changes are associated with the recent loss of Arctic sea ice'. In: *Tellus A* 62.1, pp. 1–9.

Overland, J. E. et al. (2011). 'Warm Arctic—cold continents: climate impacts of the newly open Arctic Sea'. In: *Polar Research* 30.1, p. 15787.

Overland, J. E. et al. (2016). 'Nonlinear response of mid-latitude weather to the changing Arctic'. In: *Nature Climate Change* 6.11, pp. 992–999.

Pearson, R. G. et al. (2013). 'Shifts in Arctic vegetation and associated feedbacks under climate change'. In: *Nature Climate Change* 3.7, pp. 673–677.

Pithan, F. and T. Mauritsen (2014). 'Arctic amplification dominated by temperature feedbacks in contemporary climate models'. In: *Nature Geoscience* 7.3, pp. 181–184.

Post, W. M. et al. (1982). 'Soil carbon pools and world life zones'. In: *Nature* 298.5870, pp. 156–159.

Pries, C. E. H. et al. (2012). 'Holocene Carbon Stocks and Carbon Accumulation Rates Altered in Soils Undergoing Permafrost Thaw'. In: *Ecosystems* 15.1, pp. 162–173.

Qian, H. et al. (2010). 'Enhanced terrestrial carbon uptake in the Northern High Latitudes in the 21st century from the Coupled Carbon Cycle Climate Model Intercomparison Project model projections'. In: *Global Change Biology* 16.2, pp. 641–656.

Raich, J. W. and W. H. Schlesinger (1992). 'The global carbon dioxide flux in soil respiration and its relationship to vegetation and climate'. In: *Tellus B* 44.2, pp. 81–99.

Raich, J. W. and A. Tufekciogul (2000). 'Vegetation and soil respiration: Correlations and controls'. In: *Biogeochemistry* 48.1, pp. 71–90.

Raynolds, M. K. et al. (2014). 'Cumulative geoecological effects of 62 years of infrastructure and climate change in ice-rich permafrost landscapes, Prudhoe Bay Oilfield, Alaska'. In: *Global change biology* 20.4, pp. 1211–1224.

Reich, P. B. et al. (1997). 'Nitrogen Mineralization and Productivity in 50 Hardwood and Conifer Stands on Diverse Soils'. In: *Ecology* 78.2, pp. 335–347.

Rigor, I. G. et al. (2000). 'Variations in Surface Air Temperature Observations in the Arctic, 1979–97'. In: *Journal of Climate* 13.5, pp. 896–914.

Risk, D. et al. (2011). 'Forced Diffusion soil flux: A new technique for continuous monitoring of soil gas efflux'. In: *Agricultural and Forest Meteorology* 151.12, pp. 1622–1631.

Rodwell, M. J. et al. (1999). 'Oceanic forcing of the wintertime North Atlantic Oscillation and European climate'. In: *Nature* 398.6725, pp. 320–323.

Savage, K. et al. (2008). 'A conceptual and practical approach to data quality and analysis procedures for high-frequency soil respiration measurements'. In: *Functional Ecology* 22.6, pp. 1000–1007.

Schimel, J. P. and J. S. Clein (1996). 'Microbial response to freeze-thaw cycles in tundra and taiga soils'. In: *Soil Biology and Biochemistry* 28.8, pp. 1061–1066.

Schlesinger, W. H. (1997). *Biogeochemistry: An Analysis of Global Change*. San Diego: Academic Press. 443 pp.

Schuur, E. a. G. et al. (2013). 'Expert assessment of vulnerability of permafrost carbon to climate change'. In: *Climatic Change* 119.2, pp. 359–374.

Schuur, E. A. G. et al. (2008). 'Vulnerability of Permafrost Carbon to Climate Change: Implications for the Global Carbon Cycle'. In: *BioScience* 58.8, pp. 701–714.

Schuur, E. A. G. et al. (2015). 'Climate change and the permafrost carbon feedback'. In: *Nature* 520.7546, pp. 171–179.

Screen, J. A. and I. Simmonds (2010). 'The central role of diminishing sea ice in recent Arctic temperature amplification'. In: *Nature* 464.7293, pp. 1334–1337.

Screen, J. A. and I. Simmonds (2014). 'Amplified mid-latitude planetary waves favour particular regional weather extremes'. In: *Nature Climate Change* 4.8, pp. 704–709.

Sharkhuu, N. (2003). 'Recent changes in the permafrost of Mongolia'. In: *Proceedings of the Eighth International Conference on Permafrost*. Ed. by M. Phillips et al. Lisse, Netherlands: A.A. Balkema Publishers, pp. 297–302.

Stark, J. M. and M. K. Firestone (1995). 'Mechanisms for soil moisture effects on activity of nitrifying bacteria.' In: *Applied and Environmental Microbiology* 61.1, pp. 218–221.

Stiling, P. D. (1996). *Ecology: theories and applications*. 2nd ed. Upper Saddle River, N.J: Prentice Hall. 539 pp.

Strauss, J. et al. (2013). 'The deep permafrost carbon pool of the Yedoma region in Siberia and Alaska'. In: *Geophysical Research Letters* 40.23, 2013GL058088.

Sturm, M. et al. (2001). 'Snow–Shrub Interactions in Arctic Tundra: A Hypothesis with Climatic Implications'. In: *Journal of Climate* 14.3, pp. 336–344.

Taylor, P. C. et al. (2013). 'A Decomposition of Feedback Contributions to Polar Warming Amplification'. In: *Journal of Climate* 26.18, pp. 7023–7043.

Thauer, R. K. (1998). 'Biochemistry of methanogenesis: a tribute to Marjory Stephenson:1998 Marjory Stephenson Prize Lecture'. In: *Microbiology* 144.9, pp. 2377–2406.

Verville, J. H. et al. (1998). 'Response of tundra CH4 and CO2 flux tomanipulation of temperature and vegetation'. In: *Biogeochemistry* 41.3, pp. 215–235.

Vihma, T. (2014). 'Effects of Arctic Sea Ice Decline on Weather and Climate: A Review'. In: *Surveys in Geophysics* 35.5, pp. 1175–1214.

Viovy, N. (2011). *CRUNCEP data set*. URL: ftp://nacp.ornl.gov/synthesis/2009/frescati/model_driver/cru_ncep/analysis/readme.htm (visited on 09/06/2017).

Walsh, J. E. et al. (2005). 'Cryosphere and Hydrology'. In: *Arctic climate impact assessment*. Cambdrige, New York: Cambridge University Press, pp. 183–242.

Walter, K. M. et al. (2006). 'Methane bubbling from Siberian thaw lakes as a positive feedback to climate warming'. In: *Nature* 443.7107, pp. 71–75.

Wieder, W. et al. (2016). 'CLM5.0 Tutorial 2: Running single point and regional cases'.

Wright, I. J. et al. (2004). 'The worldwide leaf economics spectrum'. In: *Nature* 428.6985, pp. 821–827.

Xiao, J. et al. (2008). 'Estimation of net ecosystem carbon exchange for the conterminous United States by combining MODIS and AmeriFlux data'. In: *Agricultural and Forest Meteorology* 148.11, pp. 1827–1847.

Zhang, T. et al. (2000). 'Further statistics on the distribution of permafrost and ground ice in the Northern Hemisphere'. In: *Polar Geography* 24.2, pp. 126–131.

Zhang, X. et al. (2013). 'Enhanced poleward moisture transport and amplified northern high-latitude wetting trend'. In: *Nature Climate Change* 3.1, pp. 47–51.

List of Figures

List of Tables

Acknowledgement

This thesis would not have been possible without the guidance and generous support of Hanna Lee, who was my supervisor during my research stay in Norway and helped me with her valuable input and feedback, and supplied me with Korean food. Furthermore, I would like to thank Yuanchao Fan for being my CLM tutor and a worthy table tennis partner, who could always help me when I encountered seemingly unsolvable programming problems.

Special thanks also go to my thesis supervisor Mag. Dr. Leopold Haimberger for his uncomplicated assistance and warm encouragement.

Lastly, I would like to thank Manuel and Simon, who have not only been my fellow students for more than five years, but have also become good friends. Maybe I would have finished my studies earlier without them, but it definitely would have been less entertaining.